M.Tech. (Computer Science) Dissertation Series

A NEW ~~THEORY~~ MODEL FOR THE EVOLUTION OF OPEN ENDED CURVES IN A TWO DIMENSIONAL PLANE (A SPECIAL CASE OF EVOLVING MANIFOLDS OF ARBITRARY CODIMENSION WITH BOUNDARIES)

A dissertation submitted in partial fulfillment of the
requirement for the M.Tech. (Computer Science)
degree of the Indian Statistical Institute

By

Saurav Basu

Under the supervision of

Dr. Dipti Prasad Mukherjee

Associate Professor

Electronics and Communication Sciences Unit

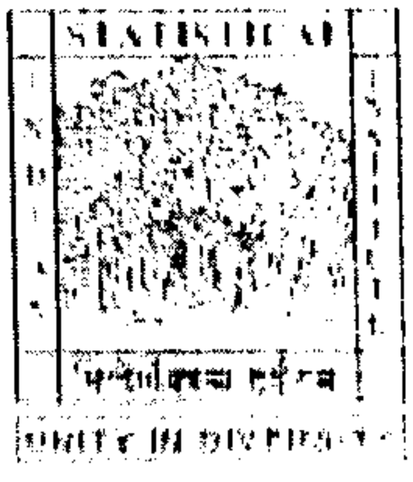

INDIAN STATISTICAL INSTITUTE
203, Barrackpore Truck Road
Kolkata 700 108

July 2005

Certificate of Approval

This is to certify that this thesis titled "A new ~~theory~~ model for the evolution of open ended curves in a two dimensional plane (a special case of evolving manifolds of arbitrary codimension with boundaries)" submitted by Saurav Basu towards partial fulfillment of requirements for the degree of M.Tech in Computer Science at Indian Statistical Institute embodies the work done under my supervision.

The dissertation report may be accepted in partial fulfillment of the requirement for the M.Tech (Computer Science) degree of Indian Statistical Institute, Kolkata, India.

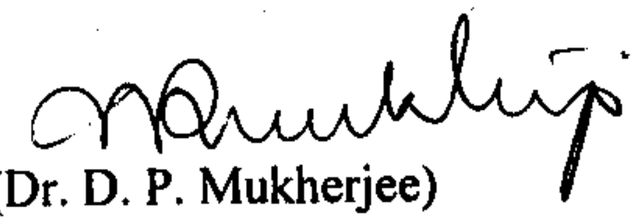

(Dr. D. P. Mukherjee)
Associate Professor
Electronics and Communication Sciences Unit
Indian Statistical Institute
Kolkata.

Acknowledgement

I would like to acknowledge and express my gratitude to all those who have supported me directly or indirectly, to complete this dissertation work.

I take this opportunity to thank my guide Dr. Dipti Prasad Mukherjee with utmost sincerity. It has been a lesson in humility and proficiency working with him. His suggestions and patience has been invaluable for completing this work.

I would also like to recall the merry hours I spent sharing the comfort of trusting companionship and unselfish guidance from the research personnel in the Atmospheric Science Laboratory in ECSU. In particular, I would like to thank Partha Pratim Mohanta, Arindam Ghosh, and N.C. Deb, who made my stay in ECSU a memory to cherish. My classmate Sudhansu Ranjan Dash, helped me immensely with his cooperation and timely anecdotes.

A special note of gratitude to all my classmates who made my stay in ISI a rewarding experience.

Saurav Basu 18/7/2005

Saurav Basu
M.Tech (Computer Science)
Indian Statistical Institute
Kolkata.

Abstract

Most of the existing mathematical theory for implicit models of manifold evolution like level set methods, focus on the evolution of hypersurfaces, i.e., codimension one motion. For example, level set methods are consistently used in the segmentation and tracking of object boundaries in medical or aerial images. This family of curve evolution works on instances of codimension one motion of a closed curve in a 2D image space. The limitation of implicit methods for evolving smooth manifolds of arbitrary codimension is a serious difficulty in segmenting shapes like blood vessels in volumetric angiogram images or roads and rivers from satellite images. The objects in previous examples are essentially one dimensional in nature and requires evolution of a curve in 3D space or that of an open-ended curve in 2D space, both of which are instances of codimension two motion.

The goal of this thesis is to build a theoretical and numerical framework to represent and evolve smooth open ended curves in a two dimensional plane, which is a special case of a manifold with boundaries and having codimension greater than one. Original ideas of the level set formulation of active contours need to be adapted to images that exhibit one-dimensional filament like structures, since, segmentation of one-dimensional filament like structures are more suitable using open ended curves rather than closed ones (classical theory of geometric active contours work only for closed curves).

We have introduced two new approaches to the problem of evolving an open-ended curve in a two-dimensional image plane. The first approach is an extension to the existing level set theory and is suitable for tracking the contours of objects in images with open curves. However, the first method essentially works for object contours that can be tracked with closed curves too. The second approach is a completely new visualization of the implicit representation of open curves in a 2D plane, and is particularly suitable for segmenting one-dimensional filament like structures in 2D images. The second approach solves a segmentation problem (of 1D filaments) that was hitherto inefficiently catered to by the traditional level set method.

We have tested the new models on both synthetic and real images that contain one-dimensional filament like structures. Results show that our models are successful in segmenting complex topological filaments with minimal distortion, and the theory is robust enough to withstand effects of shape distortions like kinks, bending, circularity and inconsistent edges and correctly approximate the shapes of the filaments. We hope to have built a novel approach to one-dimensional shape segmentation, and future work on the improvement of the models are expected to give rise to hugely efficient filament tracking algorithms encompassing a wide range of image types.

Contents

1. INTRODUCTION

Segmentation of images has been a traditional and one of the most widely investigated areas in computer vision and image processing. Segmentation subdivides an image into its constituent parts or objects. In other words, segmentation tries to extract the objects of interest (or meaningful components) from the image. For example, autonomous air-to-ground target acquisition applications may try to identify the vehicles on a road, medical applications may try to extract the thickness of blood vessels in magnetic resonance angiograms (MRA), or remote sensing applications may try to estimate the vegetation area from satellite images. One very popular way of carrying out this task of object segmentation within an image (or video sequence) is to track the contours (or boundaries) of the objects of interest with the help of some marker curves introduced by the user into the image. The marker curves are used to capture the objects of interest by evolving and aligning themselves along the boundaries of the objects, and then track the movement of the objects by propagating the marker curves along with the objects, the curves trying to mimic the object boundaries all the time. These marker curves are called *active contours* or s*nakes* in computer vision literature.

1.1 IDEA BEHIND THE ACTIVE CONTOUR MODEL

Active contours (or *snakes*) are curves defined within an image domain that move with time through the image space under the influence of internal forces generated within the curve trying to balance external forces generated by the image data. Often the internal and external forces are defined in such a way that they exactly balance at the edges of object boundaries within the image. This results in the ceasing of movement of the active contours at object edges, thus capturing the object boundary(s) and segmenting the object. A very common practice is to initialize a closed contour around an object to be detected, and evolving the curve until it stops at the object boundary. The final shape of the contour denotes the boundary of the object.

There are two active contour models prevalent in the literature today, *parametric active contours* and *geometric active contours*. Parametric models represent a curve parametrically, the parameter generally being the arc-length of the curve. They solve a parametric time-dependent partial differential equation incorporating the contribution of internal and external forces, getting the new parameterization of the curve at the next time instant. This explicit scheme of tracking the curve points at every time instant suffers from problems like loss of resolution of the tracked points along places, instability of the numerical schemes due to large sensitivity to distance between tracked particles, and inability to elegantly handle topological changes.

Geometric active contour models avoid the explicit tracking of curve points by implicitly describing the curve as some subset of a higher dimensional function described over the image domain. The model then evolves this higher-dimensional function with time to track the movement of the curve. For example, in the level set method, the evolving closed curve within the 2D image is expressed as the zero level set of a 3D surface defined suitably. The evolution of this surface with time is used to track the movement of

the zero level set, which, in our case, is the desired curve. The implicit models do not suffer from the lack of numerical stability, loss of resolution, and can elegantly handle topological changes like joining and breaking of curves. The only compromise, to a certain extent, may be the speed of the algorithm, since instead of a few curve points, we now update a function defined over the whole image matrix.

1.2 DEFICIENCY IN THE GEOMETRIC ACTIVE CONTOUR MODEL AND OUR MOTIVATION

Most of the applications of, and existing mathematical theory for implicit models like level set methods, however, focus on the evolution of hypersurfaces, i.e., *codimension*[1] one motion. For example, level set methods are consistently used in the segmentation and tracking of object boundaries in 2D medical or aerial images [5,8,9]. This family of curve evolution works on instances of codimension one motion of a closed curve in 2D space. The limitation of implicit methods for evolving smooth manifolds of arbitrary codimension is a serious difficulty in segmenting shapes like blood vessels in volumetric angiogram images or roads and rivers from satellite images. The objects in the previous examples are essentially one dimensional in nature and requires evolution of a curve in 3D space or that of an open-ended curve in 2D space, both of which are instances of codimension two motions. Thus, one would like to develop ideas to extend the classical implicit geometric contour theories to real life segmentation problems in codimension two cases.

Recent work in differential geometry has developed equations necessary to evolve arbitrary dimensional manifolds in arbitrary dimensional space using level set methods [1]. These have been applied to the evolution of one-dimensional infinite (or closed) curves in three-dimensional space, as in the case of segmenting blood vessels in volumetric magnetic resonance angiography images [4]. Mathematical framework for motion of one-dimensional infinite (or closed) curves in three-dimensional space has also been developed independently by Burchard [2]. A diffusion-generated motion by mean curvature for filaments also addresses the same problem by resorting to a modified form of the Complex Ginzburg-Landau equation [6]. All of the above extensions of the level set method to handle the arbitrary co-dimension case work satisfactorily for evolving infinite (or closed) curves in $\Re^3$, but handling open-ended curves in 2D evolving space still remains a niche area. Such necessities, for example, may arise, in segmenting a road network or river course from a satellite image, where, the object to be segmented has an essentially one-dimensional filament-like structure. Other applications may include evolving an open-ended curve in feature space to generate a non-linear boundary between the different pattern classes.

1.3 OUR PROPOSED APPROACH

The goal of this research is to build a theoretical and numerical framework to represent and evolve *smooth* open ended curves in a two dimensional plane, which is a special case

[1] Codimension of a manifold in the context of an embedding is defined as the difference between the dimension of the manifold and the dimension of the evolving space. It is described in greater detail in the next chapter.

of a manifold with boundaries and having codimension greater than one. Original ideas of the level set formulation of active contours need to be adapted to images that exhibit one-dimensional filament like structures. Segmentation of one-dimensional filament like structures are more suitable using open ended curves rather than closed ones. The overall contribution of our work can be summarized as

- Developing a new implicit representation of open-ended curves in 2D.
- Establishing a mathematical model for the time evolution of the implicit representation that consequently evolves the open-ended curves in 2D (codimension greater than one).
- Applying the new model to segment one-dimensional structures in real 2D images by open-ended curves.

The models proposed in the thesis try to create a theoretical and mathematical framework for the evolution of open-ended curves in a two-dimensional image domain. The first model tries to extend the work of Zhao of evolving junctions in multiphase interface motions using level sets [11], and visualizes an open-ended curve as the intersection of the zero level sets of two closed curves. The constraint for such evolution is the synchronization of velocities at the zero level set intersections

The second model visualizes the open-ended curve as the medial axis of the level set of a function (named as the *curvature map*) defined on the curve. The level set is allowed to undergo a mean curvature motion. This *approximately* evolves the medial axis of the level set according to its curvature between the end points and tries to elongate the medial axis at the end points in a tangential direction. The elongated medial axis is taken as the updated position of the curve and the calculations repeated for finding out the subsequent positions of the curve.

1.4 ORGANIZATION OF THE REPORT

This report develops the ideas presented above through the following sections. Chapter 2 reviews basic level let theory and related attempts in extending codimension one motion of the level sets to evolution of smooth manifolds of arbitrary codimension. Chapter 3 introduces our models with the mathematical explanations and their logical justifications. Chapter 4 presents the results of applying our numerical model to various synthetic and real images, with different types of contours and shapes. Chapter 5 addresses the need to establish the idea presented by our model by rigorous mathematical results, and is followed by the conclusion.

2. BACKGROUND AND RELATED WORK

In order to clarify the deficiency of existing implicit curve evolution models, we need to understand the mathematical implications of these models and the specific points where they lack generalization capabilities. We therefore give a brief overview of the existing mathematical work in the area of implicit models for evolution of manifolds of arbitrary codimension and point out their problems in the context of our goal of evolving open-ended curves in 2D. The variety of approaches of the following methods (outlined in sections 2.1, 2.2, 2.3 and 2.4) and the related difficulties are expected to give an idea to the reader about the numerical subtlety and the complexity of the problem that we propose to solve.

Given below is a brief description of some basic terminologies, basic level set theory and its extensions to problems of higher codimensions.

2.1 DIFFERENTIAL GEOMETRY TERMS AND ACTIVE CONTOURS

Manifold

A m*anifold* of dimension n is a set M and a family of injective mappings $\phi_i : \Omega_i \subset \Re^n \rightarrow M$ of open sets Ω_i of $\Re^n$ into M such that

- $\cup_i \phi_i(\Omega_i) = M$
- For any pair (ϕ_i, ϕ_j), if $W = \phi_i(\Omega_i) \cap \phi_j(\Omega_j) \neq O$ (O denotes the null set), then the sets $\phi_i^{-1}(W)$ and $\phi_j^{-1}(W)$ are open and the function $\phi_i^{-1} o \phi_j$ is differentiable.

For example, a *curve* embedded in a plane, can be represented as a mapping $\phi : [a, b] \rightarrow \Re^2$, of dimension one, where $[a, b] \subset \Re$. *Closed curves* have the additional property, $\phi(a) = \phi(b)$ (In case $\phi(a) \neq \phi(b)$, the curve has endpoints and is hence called an *open curve*). We assume the curve to be a closed curve for this example. For this same curve embedded in 3D space, we can use another mapping $\theta : [a, b] \rightarrow \Re^3$, where, with the preceding example of the closed curve, we have, $\theta(a) = \theta(b)$.

Codimension

Codimension of an embedding is the difference in dimensions between the higher dimensional manifold and the lower dimensional manifold involved in the embedding. Let us illustrate this point with more details. In the previous example of the closed curve (which we call a manifold of dimension one since it is a mapping from the set $\Re$), the curve is embedded in a plane (which can be thought of as a mapping from $\Re^2$ to $\Re^2$, and

hence a manifold of dimension two), so the codimension for this embedding is equal to two-one=one. If we consider the same curve embedded in 3D space, then the space can be thought of as a mapping from $\Re^3$ to $\Re^3$, hence a manifold of dimension three, and the codimension becomes three-one=two. Again, if we consider an open curve embedded in the plane, then, this open curve can be thought of as a 1D curve bounded by two points of dimension zero at its ends, hence the codimension of the embedding of the end points on the plane is two-zero=two, whereas the codimension of the embedding of the curve (between the end-points) remains one. If we consider the same open-ended curve embedded in 3D space, then the codimension of the end-points become three-zero=three, and that of the curve (between the end-points) remains two.

Closed curve evolution theory

In most cases, the closed curve C is given as a mapping of the normalized arc-length s, so that, we can define our 2D image as a mapping $u_0 : \Re^2 \to \Re$, and our parameterized closed curve as $C(s) : [0,1] \to \Re^2$, where $C(0) = C(1)$. For a closed curve that is evolving with time (or changing shape over time, while staying a closed curve), we generally term it as an *active contour* and we have the Partial Differential Equation describing its motion as [8]:

$$C_t(s,t) = v(s,t)\mathrm{N}(s,t) \tag{2.1}$$

where,

i) $C(s,t)$ is the explicit representation of the curve with the 1D parameter s, and t is time (in terms of the definition of the manifold, C is a 1D manifold with the mapping $C : [0,1]\times[0,t) \to \Re^2, [0,1] \subset \Re$). $C_t(s,t)$ stands for partial differentiation of $C(s,t)$ with respect to time[2]).

ii) $\mathrm{N}(s,t)$ is the unit vector in the normal direction to the curve point $C(s,t)$.

iii) $v(s,t)$ is the magnitude of the velocity of the curve in the direction of $\mathrm{N}(s,t)$.

We have considered $C(s,t)$ to be a smooth and continuous curve and neglected the deformation of the curve in the tangential direction, since tangential velocity only serves to re-parameterize the curve [8].

The main task at hand is to estimate the normal velocity v(s, t) so that the curve deforms and ultimately stops at the boundary of the object. The same problem can be approached from an energy minimization principle, where we try to minimize the energy functional [10]

[2] A subscript variable will mean a partial differentiation with respect to that variable throughout this report, unless otherwise stated or another meaning is very evident from the context.

$$I(C) = \alpha \int_0^1 |\frac{\partial C}{\partial s}|^2 \, ds + \beta \int_0^1 |\frac{\partial^2 C}{\partial s^2}|^2 \, ds + \lambda \int_0^1 | f(|\nabla u_0(C(s))|)^2 \, ds \qquad (2.2)$$

where, α, β, λ are positive parameters. The first two terms control the snake's tension and rigidity respectively, and the third term denotes a function of the image gradient ∇u_0 that takes on smaller values at the object boundary. The Euler-Lagrange equation for (2.2) has the following form [10]:

$$C_t(s,t) = \alpha \frac{\partial^2 C}{\partial s^2} - \beta \frac{\partial^4 C}{\partial s^4} - \nabla f(|\nabla u_0(C(s))|) \qquad (2.3)$$

which is analogous to equation (2.1).

2.2 INTRODUCTION TO THE PROBLEM OF OPEN CURVES WITH REFERENCE TO BASIC LEVEL SET MOTION

We now elaborate the basic level set methodology and its fundamental shortcomings.

2.2.1 BASIC LEVEL SET THEORY AND MEAN CURVATURE MOTION

The level set method and in particular the motion by mean curvature of Osher and Sethian [9] approaches the parametric curve evolution problem stated in equations (2.1) and (2.3) as follows:

Let Ω be a bounded open subset of $\Re^2$, with $\partial\Omega$ as its boundary.

We define a 2D Lipschitz function (surface, if we prefer geometric terms) $\phi(x,y,t)$, $\phi : \Re^2 \times [0,t) \to \Re$, over the plane of interest, such that at each instant, $S = \{(x,y) \mid \phi(x,y,t) = 0\}$ is same as $L = \{(x,y) \mid C(s,t) = [x(s,t), y(s,t)]\}$. Or in other words, the *zero level set*[3] of ϕ at each instant coincides with C. Now, in case of the level sets of ϕ, $\phi(x,y,t) =$ a constant. Taking the derivative on both sides of $\phi(x,y,t) =$ constant with respect to t, and noting that $V(s,t) = v(s,t)\mathrm{N}(s,t)$ ($V(s,t) = v(s,t)\mathrm{N}(s,t)$ is analogous to the form $C_t(s,t) = v(s,t)\mathrm{N}(s,t)$ in equation (2.1)), we have,

$$\nabla\phi V(s,t) + \phi_t = 0,$$

or, $\phi_t = -\nabla\phi V(s,t) = -v(s,t)\nabla\phi N(s,t)$.

Since $N(s,t) = \frac{\nabla\phi}{|\nabla\phi|}$ at the level sets, we get,

[3] Zero level set of any function f is the set of points $\{\mathbf{x}\}$ for which $f(\mathbf{x})=0$.

$$\phi_t = -\nu(s,t)\,|\nabla\phi| \tag{2.4}$$

For the case when the curve in equation (2.4) moves with a speed that is proportional to its curvature as well as the function f (f is stated in equations (2.2), (2.3)), equation (2.4) may be concretely stated as –

$$\phi_t = -f(|\nabla u_0|)\,|\nabla\phi|\,(div(\frac{\nabla\phi}{|\nabla\phi|}) + \varepsilon) \tag{2.5}$$

since, curvature $= div(\frac{\nabla\phi}{|\nabla\phi|})$ and, $\varepsilon \geq 0$ is a constant. Also, we have, $\phi(x,y,0) = \phi_0$ as the initial level set function.

This level set function ϕ is chosen in such a way that the zero level set of this function can be extracted in a precise and efficient manner. The most popular choice is a function that is defined positive (or negative) inside the closed curve, and negative (or positive) outside it, so that the curve lies at the zero crossing (or zero level set) of the function and is easy to locate numerically. Mathematically,

$$\begin{cases} C = \partial\omega = \{(x,y) \in \Omega : \phi(x,y) = 0\}, \\ inside(C) = \omega = \{(x,y) \in \Omega : \phi(x,y) > 0\}, \\ outsise(C) = \Omega/\omega = \{(x,y) \in \Omega : \phi(x,y) < 0\} \end{cases} \tag{2.6}$$

$\partial\omega$ represents the boundary of the region $\omega \subset \Re^2$ and ϖ denotes the complement of ω in equation (2.6). The commonest form of the function ϕ is taken as the signed distance function to the closed curve C, such that $|\nabla\phi|=1$. This form of the level set function ensures that there are no sharp gradients developing in the level set function during computation (sharp gradients render the computation numerically unstable). Also, a signed distance function makes the zero crossing of the level set smooth and easily locatable.

2.2.2 PROBLEMS WITH OPEN CURVES AND MANIFOLDS OF ARBITRARY CODIMENSION IN GENERAL

In equation (2.5), in order to find the level set for $\phi(x, y, t)$, it is necessary that the x-y plane intersects $\phi(x, y, t)$ in distinct points, which means that there must be zero-crossing in $\phi(x, y, t)$. I.e., there must be distinct regions in the plane in which $\phi(x, y, t)$ either lies below the plane (i.e., negative), or above the plane (i.e., positive). So, it is important for the curve to divide the plane into distinct, bounded regions so that $\phi(x, y, t)$ can be defined to be positive in one region and negative in another region. In mathematical

terms, the manifold with the lower dimension should partition the manifold with the higher dimension into separate regions, which in the case of the closed curve becomes the region "inside" the curve and the region "outside" the curve.

But, this division into inside/outside regions *cannot* be obtained in case of embeddings with codimension greater than one. For example, in case of an open curve in a plane, the maximum codimension of the embedding is two, when we consider the end points of the curve having dimension zero being embedded in the plane with dimension two (with the resultant codimension being two minus zero = two). Thus, the open curve cannot divide the plane on which it lies into separate regions, and hence we cannot define a similar scalar distance function with zero crossing in this case. A distance function must be everywhere positive, and is thus, singular on the curve itself. Same is the case for any embedding with arbitrary codimension greater than one.

The problems in evolving a level set function ϕ whose zero level set is not a zero crossing of the function might be numerous. Numerical errors may accumulate and it may be numerically impossible to calculate the gradient at the zero level set (if the function is singular there) or impossible to locate the zero magnitude points. For image processing applications such numerical instability may lead to a complete collapse of the segmentation algorithms. Also, the notion of mean curvature motion is undefined in case of open curves as curvature itself is undefined at the endpoints of the open curve. The familiar theory of geometric active contour based segmentation of images with curves that moved under mean curvature motion fails in case of open curves.

Clearly, some other way of implicitly visualizing the open-ended curve in a level set framework has to be developed. We give below some ideas of evolving an open curve by extending the theory of level sets (applicable to hypersurfaces, i.e., embeddings with codimension one) to open ended curves (an embedding with codimension two at the endpoints).

2.3 EXISTING WORK FOR THE EVOLUTION OF MANIFOLDS WITH ARBITRARY CODIMENSION

We now give below some mathematical work aimed at evolving smooth manifolds of arbitrary co-dimensions, and more specifically co-dimension two manifolds, in the level set framework. The principal emphasis here is to evolve closed (or infinite) curves in $\Re^3$ or three-dimensional Euclidean space.

2.3.1 LEVEL SET APPROACH TO MEAN CURVATURE FLOW IN ARBITRARY CODIMENSION (AMBROSIO AND SONER, 1996 [1])

For a smooth manifold C evolving in a space of dimension d and of codimension $(d\text{-}k)$ (i.e., with a dimension k), we can define an auxiliary smooth Lipschitz function $u : \Re^d \to \Re$ so that the zero level set Γ of this function at all times is equal to our manifold C.

$$\Gamma = \{x \in \Re^d : u(x,t) = 0\} \tag{2.7}$$

We have to choose an initial u_0 such that,

$$\Gamma_0 = \{x \in R^d : u_0(x) = 0\} \tag{2.8}$$

In order to evolve Γ according to its mean curvature, its principal curvatures are expressed in terms of the derivatives of this auxiliary function u. If $k \geq 1$, then as we have stated earlier in section 2.2.2, $u \geq 0$, and $|\nabla u|$ vanishes on Γ. Therefore, instead of Γ, the ε-level set[4] of Γ, or Γ^ε, for small $\varepsilon > 0$ is considered for evolution. Figure 2.1(a) shows an open curve C and the associated Γ^ε. Since Γ is assumed to be smooth, u may be chosen such that $|\nabla u|$ does not vanish on Γ^ε for small $\varepsilon > 0$. A projection matrix $J(u)$ is defined as the symmetric $d \times d$ matrix

$$J(u) = \frac{1}{|\nabla u|} P_{\nabla u} \nabla^2 u P_{\nabla u}, \quad P_p = I - \frac{p \otimes p}{|p|^2}, p \neq 0, \tag{2.9}$$

that projects any d dimensional vector into the normal space of $|\nabla u|$ ($\otimes$ denotes the tensor product and I denotes the identity matrix). Let, $\lambda_1(J) \leq \lambda_2(J) \leq .... \leq \lambda_d(J)$ be the *eigenvalues of J(u). We have the following properties of these eigenvalues:*

i) *0 is an eigenvalue corresponding to the eigenvector ∇u.*

ii) Other (d-1) eigenvalues are equal to the principal curvatures of the codimension one surface Γ^ε.

iii) For small ε, keeping in mind that the codimension of Γ is k, we expect Γ^ε to have very large (k-1) principal curvatures, and the remaining d-k principal curvatures to be very close to the principal curvatures of Γ.

As $\varepsilon \downarrow 0$,

$$\sum_{i-1}^{d-k+1} \lambda_i(J) \tag{2.10}$$

converges to the mean curvature of Γ. Given an initial data Γ_0, a scalar function $u_0 : \Re^d \to [0, \infty)$ satisfying equation (2.8) is chosen, and the function is evaluated according to the update equation

$$u_t = \sum_{i-1}^{d-k+1} \lambda_i(J(u)) \tag{2.11}$$

---

[4] The ε-level set for any function f is defined as the set of points {x} for which f(x)= ε.

which is an evolution equivalent to evolving the manifold Γ according to

$$\Gamma_t = \kappa \vec{N} \tag{2.12}$$

(where κ is the mean curvature of Γ, and $\vec{N}$ is the unit normal vector to Γ) because, Γ is the zero level set of u throughout the evaluation. The ε level sets of u, when ε is very close to zero, define thin tubes around Γ, which evolve correctly according to the mean curvature of Γ. Figure 2.2 shows a thin tube initialized around the manifold Γ that is evolving under mean curvature motion. The bumps of the tube in figure 2.2 is first smoothed out until the shape approximates a torus, then the torus shrinks to a point.

The problems with this approach are many. The recovery of the manifold from the zero level set of u is numerically difficult. Sensitivity to noise in the image data when this procedure is used to evolve one-dimensional thin tubes in a three dimensional image may destroy the shape of the thin tubes. Hence visualizing and extracting the zero level set as the medial axis of these thin tubes may not be possible. In other words, when the evolution of the curve is proportional to mean curvature only, medial axis of the tubes faithfully represent the curve, but any image driven data may distort the shape of the tubes considerably so that their medial axis deviates from the evolving manifold. Also, this procedure is undefined in the case of evolving a manifold with boundaries, as for example our primary interest in the open ended curve where the boundaries are the two end points, or the case of a surface patch evolving in a three dimensional space where the boundary is the perimeter of the patch. Both these boundaries represent a codimension two embedding, but this method fails here as the mean curvature is undefined at the boundaries. This work has been extensively used in segmenting blood vessels in 3D magnetic resonance angiography (MRA) images [4], but the evolving manifolds are infinitely long thin tubes in these cases, without any endpoints.

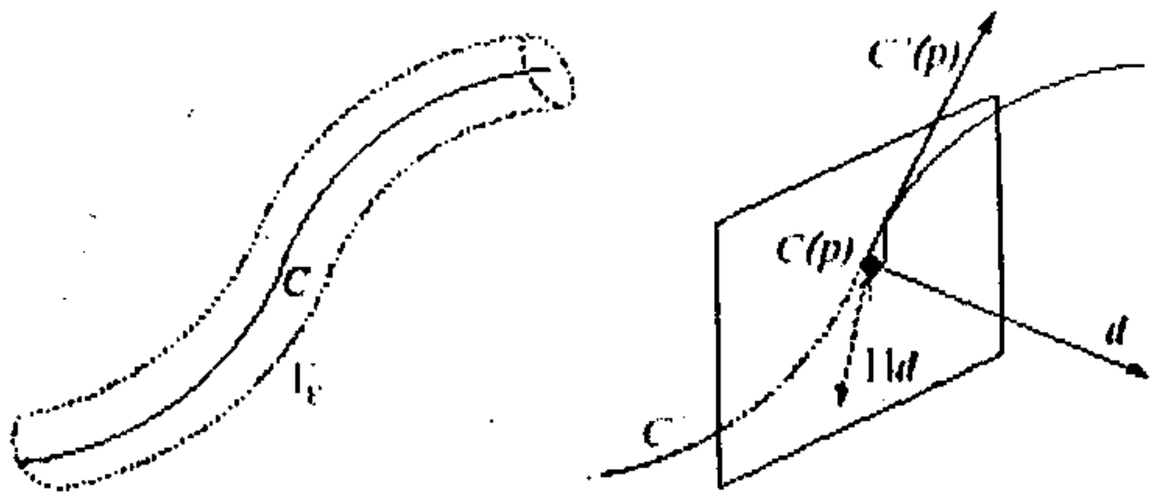

(a) (b)

Figure 2.1: A codimension-two curve. (a) Tubular iso-level set Γ^{ε} of C. (b) The tangent to C at p, the normal plane, an external vector $\vec{d}$ which comes from image data, and its projection onto the normal plane [4].

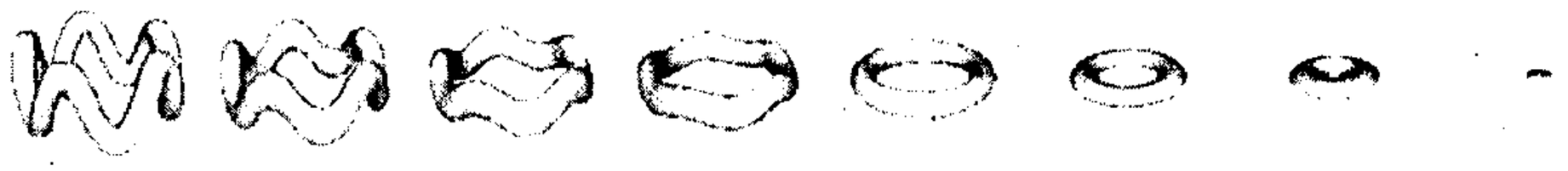

Figure 2.2: Tubular object evolving under mean curvature motion to smooth the underlying curve. The bumps are first smoothed out until the shape approximates a torus, then the torus shrinks to a point [4].

2.3.2 MOTION OF CURVES IN THREE SPATIAL DIMENSIONS USING THE INTERSECTION OF TWO HYPERSURFACES (BURCHARD, CHENG ET AL. 2001 [2])

Hypersurfaces are embeddings that have codimension one. For example, a closed curve in a two dimensional plane is a hypersurface as its codimension or the difference between the dimension of the evolving space (two in this case for the plane) and the curve (one in this case) is one.

In this approach, a bi-dimensional vector function is used to represent and evolve a curve C in $\Re^3$, or more specifically, two separate level set functions are used whose intersection represents the curve. We give below the mathematical framework of the model.

Suppose, we have a curve C in $\Re^3$ that evolves by the normal directional motion as in equation (2.1),

$$C_t = v\vec{N}, \tag{2.13}$$

where, v is the speed in the normal direction $\vec{N}$ to the curve. We can define two Lipschitz functions $\phi : \Re^3 \times [0,t) \to \Re$ and $\psi : \Re^3 \times [0,t) \to \Re$ such that, the intersection of their zero level sets represent the curve. In other words,

$$C = \Gamma_1 \cap \Gamma_2, \text{ where, } \Gamma_1 = \{(x,y) \mid \phi(x,y,t) = 0\} \text{ and } \Gamma_2 = \{(x,y) \mid \psi(x,y,t) = 0\} \tag{2.14}$$

Figure 2.3 shows the curve depicted in equation (2.14), where, a segment of a circular helix C in R^3 is represented as the intersection of the zero level sets of the two hypersurfaces $\phi = 0$ and $\psi = 0$ Thus, the one-dimensional curve C is formed by the intersection of the hypersurfaces represented by the zero level sets of ϕ and ψ. The evolution of C is carried out by indirectly evolving the two hypersurfaces ϕ and ψ separately, taking appropriate steps to guarantee that the intersection of the zero level sets

of this curve coincides with C at all times. Thus, in order to evolve C with a velocity $\vec{v}$, the two hypersurfaces are evolved according to the familiar level set equations -

$$\begin{cases} \phi_t + \vec{v} \circ \nabla \phi = 0 \\ \psi_t + \vec{v} \circ \nabla \psi = 0 \end{cases} \tag{2.15}$$

The velocity field $\vec{v}$ is now defined over the whole of $\Re^3$, and $\circ$ denotes the vector dot product.

This method suffers from some serious limitations. Initialization of the level sets ϕ and ψ in all of $\Re^3$ to form the desired curve at their intersections is a complicated task. Though forming these functions close to the desired curve is easy, these local constructions cannot be easily extended to the whole of $\Re^3$, causing problems during topological changes. More importantly, this method is unable to handle the specific case we are interested in, i.e., the case of an open ended curve, or more generally a manifold with a boundary.

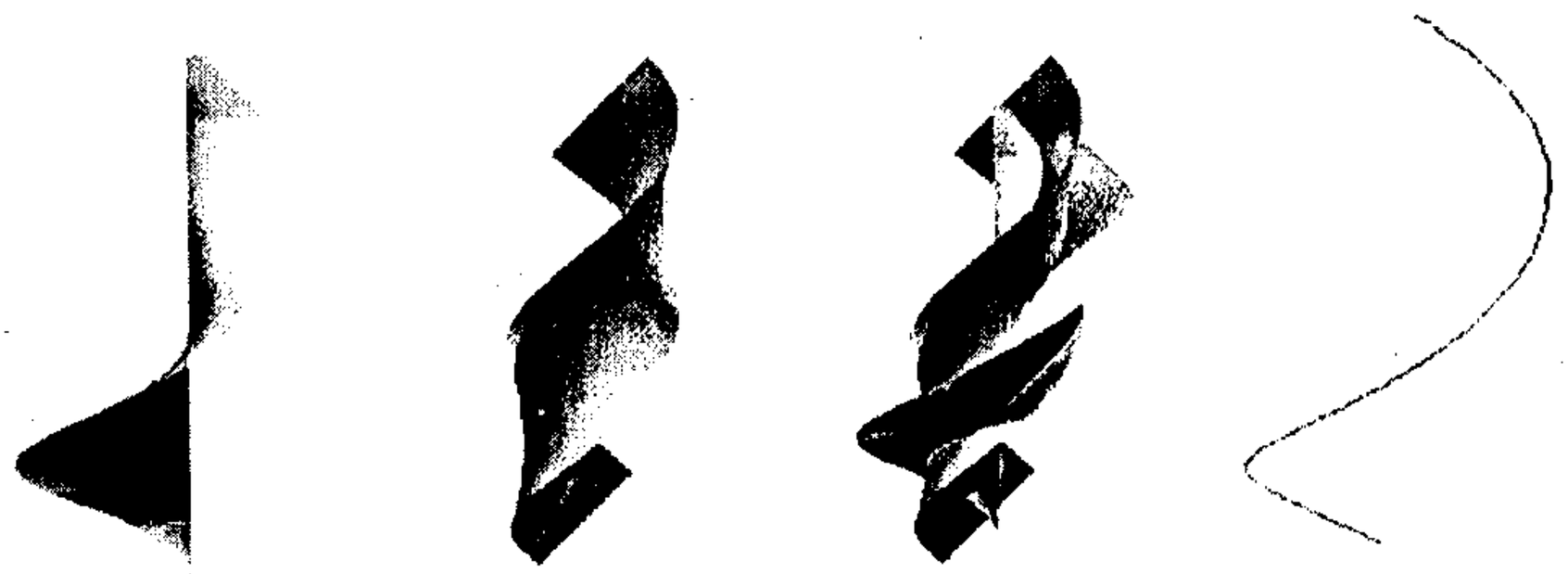

$\phi = 0$ $\psi = 0$ $(\phi = 0) \cap (\psi = 0)$ $C = (\phi = 0) \cap (\psi = 0)$

Figure 2.3: A segment of a circular helix C in R^3 is represented as the intersection of the zero level sets of the two hypersurfaces $\phi = 0$ and $\psi = 0$ [3].

2.3.3 DIFFUSION GENERATED MOTION BY MEAN CURVATURE FOR FILAMENTS (RUUTH, MERRIMAN ET. AL, 1998 [6])

This model is inspired by the simple and robust diffusion-generated motion algorithm for producing motion by mean curvature of a hypersurface [6], and it attempts to generalize this algorithm from hypersurfaces to the motion by curvature of a curve in three dimensions. It takes the help of the *Complex-Ginzberg-Landau* equation

$$u_t = \nabla^2 u - \frac{1}{\varepsilon^2} u(|u|^2 - 1) \tag{2.16}$$

where $u(x,t)$ is a complex scalar and $0 < \varepsilon << 1$. The equation is a basic model for understanding the motion of phase defects (singularities). For $x \in \Re^3$ the defects are generally supported on a one-dimensional curve (filament) where $|u^\varepsilon|$ vanishes. Asymptotic analysis of equation (2.16) for the case $\varepsilon \to 0$ shows that for any initial data $u(x,0)$ vanishing on a filament Γ_0 and having a *winding number*[5] one around it, the solution of equation (2.16) leads to a complex scalar vanishing along the filament Γ_t which is generated from Γ_0 as motion by curvature along the normal.

This procedure, called the **Complex-Diffusion-Generated-Motion** (CDGM) applies a formal splitting procedure to the complex *Ginzberg-Landau* equation to produce a motion of filaments by their mean curvature. The algorithm is given below –

ALGORITHM **CDGM**

GIVEN: An initial filament in $\Re^3$.

BEGIN:

(1) *Initialize*: Set χ (a complex function defined over $\Re^3$) so that its "centre of winding" coincides with the filament. I.e., set $\chi(x)$ ($x \in \Re^3$) so that its winding number with respect to zero in the complex plane is nonzero when x moves around any closed loop that encircles the filament.

(2) *Repeat for all steps*:

a) *Normalize:* $\chi_t = -\frac{1}{\varepsilon^2} \chi(|\chi|^2 - 1)$ (2.17)

This reaction step reduces to its formal limit for $\varepsilon \to 0$ to a simple normalization step

$$\overline{\chi} = \frac{\chi}{|\chi|} \tag{2.18}$$

b) *Diffuse:* Starting from $\overline{\chi}$, evolve χ for a time Δt according to

---

[5] *Winding number* of a contour γ about a point z_0 is defined as the number of times the contour γ passes counterclockwise around the point z_0.

$$\chi_t = \nabla^2 \chi \tag{2.19}$$

END

The location of the interface Γ_t is given by the zero contour of χ.

The same problems persist of locating the curve accurately since it is defined as a singular set of a function and is a drawback when dealing with sampled functions. Moreover, it does not handle our problem of interest, i.e., an open-ended curve in the two-dimensional plane, and is generally valid for infinitely long curves in $\Re^3$. Moreover, application of this procedure in segmentation of real images has been very few.

2.3.4 THE VECTOR DISTANCE FUNCTION APPROACH (JOSE GOMES, 2001 [3])

This method approaches the problem of evolution of manifolds of arbitrary codimension from a radically different perspective. Rather than viewing the manifold of interest as the zero level set of a scalar function, it represents the manifold as a zero level set of a vector function called the ***Vector Distance Function*** (VDF). It then tries to evolve the vector function with the help of a vector partial differential equation.

Let us consider a smooth manifold $\Im$ of codimension k in $\Re^n$ such that $\Im : \Re^{n-k} \times [0,T) \to \Re^n$, and, let it evolve according to the time evolution equation:

$$\begin{cases} \Im_t(p,t) = \vec{v} \\ \Im(\cdot,0) = \Im_0 \end{cases}, \tag{2.20}$$

where, $p \in \Re^{n-k}$, and $\vec{v}$ (defined all over $\Re^n$) is the projection of an n dimensional velocity field in the normal space of the manifold of interest $\Im(p,t)$. $\vec{v}$ is piecewise smooth, and contains contributions from both the geometric properties of the manifold (such as curvature) and external force fields (arising from image data). This method defines an auxiliary mapping $u : \Re^n \times [0,T) \to \Re^n$ such that $u(\Im(p,t),t) = 0$, and the manifold is defined as $\Im = u^{-1}(0)$. This mapping is called the ***Vector Distance Function*** [3], and is defined as the gradient of the squared distance function to a given manifold. Mathematically, if δ be the scalar distance function to a given manifold $\Im$, such that $|\nabla \delta| = 1$, then the vector distance function u is defined as:

$$u = \nabla\left(\frac{\delta^2}{2}\right) \tag{2.21}$$

The reader is advised to refer to figures 2.4, 2.5 and 2.6 to get a feel of the vector distance functions of some regular geometric shapes. The characteristic equation for the family of vector distance functions is given by

$$(Du)^T u = u, \tag{2.22}$$

where Du denotes the spatial derivative of the vector u in $\Re^n$ in equation (2.22) and is an $n \times n$ matrix, and T denotes the transpose operator. It can be shown that the family of solutions of equation (2.20) can be obtained implicitly by considering the following system of partial differential equations

$$\begin{cases} u_t(x,t) = b(x,t) \\ u(\cdot,0) = u_0 \end{cases}, \tag{2.23}$$

where, $b : \Re^n \times [0,T) \to \Re^n$ is another vector field called the *velocity-vector-field* that satisfies the following first order, quasi-linear partial differential equation

$$(Db)u = (I - Du)b, \tag{2.24}$$

with initial conditions

$$b(\Im(p,t),t) = -v(\Im(p,t),t), p \in \Re^{n-k} \tag{2.25}$$

wherever u is defined and differentiable. The evolution is designed such that u remains the gradient of the squared distance function to $\Im(p,t)$ as in equation (2.21).

The main problem of this method is the absence of stable and generic numerical schemes for the governing partial differential equations (2.23) and (2.24). The main issue is to cope efficiently with the nonlinearity of the underlying problem. Moreover, incorporation of complex velocity fields from image segmentation models makes the initial conditions in equation (2.24) almost impossible to implement. Though this scheme mathematically incorporates cases of manifolds with boundaries, like our open-ended curve in a two-dimensional plane, it is unclear how to efficiently arrive at a stable numerical scheme to solve equations (2.23) and (2.24). The theory of VDF is still in a formative stage and has hardly been used to segment real 2D or 3D images.

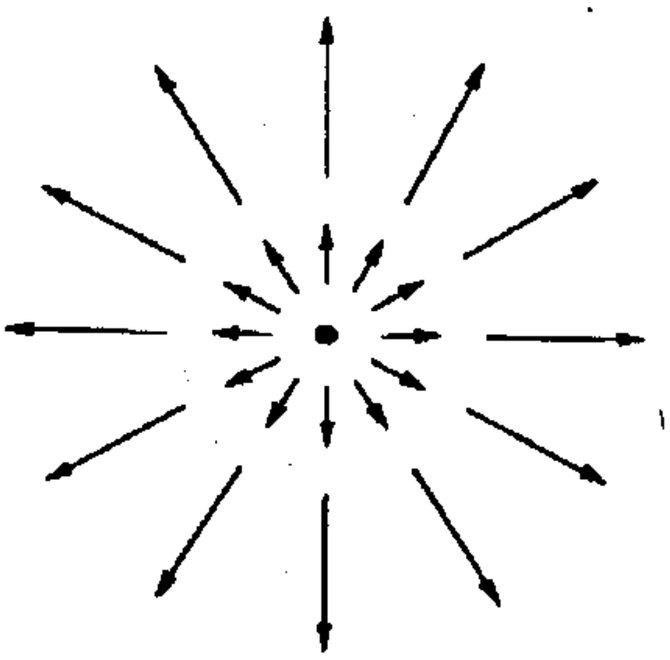

Figure 2.4: The VDF of a point: a radial field equal to zero at the point [3].

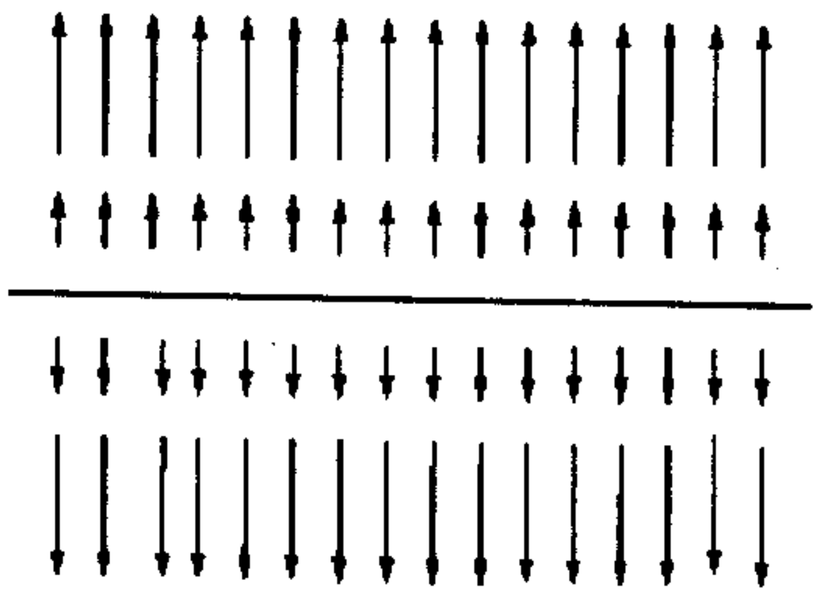

Figure 2.5: The VDF of a line: a field equal to zero on the line [3].

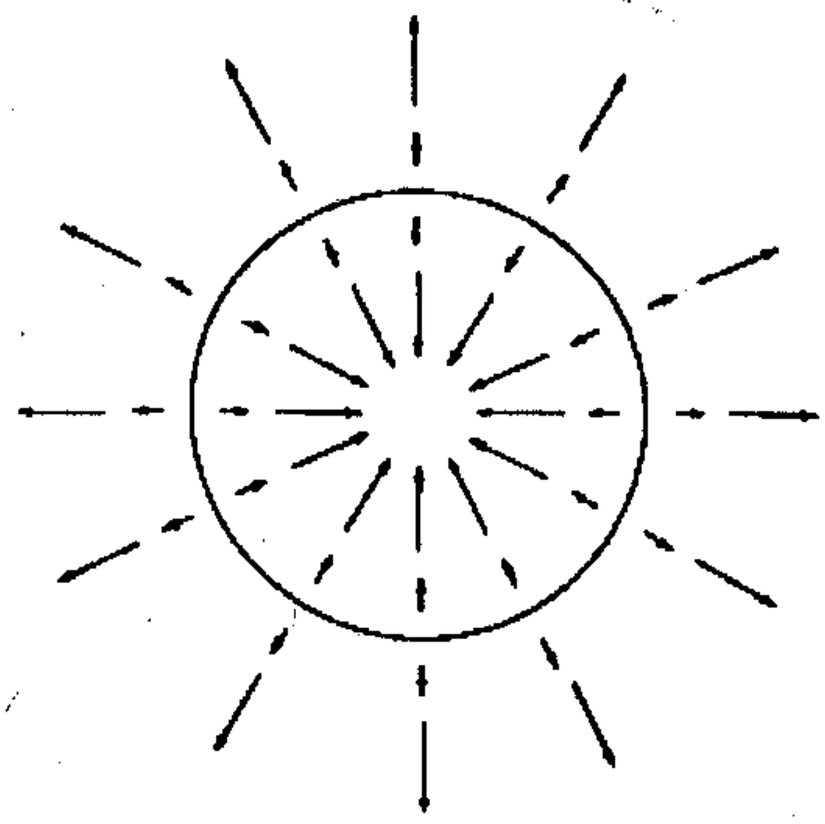

Figure 2.6: The VDF of a circle: a radial field equal to 0 on the circle and undefined at the center [3].

2.4 SCOPE AND NECESSITY OF DEVELOPMENT OF MODELS FOR OPEN-ENDED CURVES AND OUR RESEARCH MOTIVATION

The description of the existing models in section 2.3 should be enough to point out the necessity of developing an implicit model for open-ended curves. Our interest lies principally in the 2D domain, because we estimate that segmentation of one-dimensional structures in two-dimensional images is going to be a very important necessity in the bio-medical domain and defense applications. Segmentation of blood vessels and nerve interconnections in MRI images and the automatic tracking of river/road networks from satellite images should be a very challenging and helpful achievement for the medical fraternity and defense organizations. Thus, we proceed to develop our model for the evolution of open-ended curves in the 2D plane in the next chapter.

3. DESCRIPTION OF THE PROPOSED MODELS

We attempt to tackle the problem of defining suitable higher dimensional functions for describing curves having codimension two or more by venturing in two separate directions. We follow the direction introduced by [11] in extending the movement of multiple junctions in creating a model, which interprets an open-ended curve as a junction between two closed curves, and consequent movement of the junction by the simultaneous and synchronized movement of both the level sets.

The second model visualizes the open-ended curve as the medial axis of the level set of a function defined on the curve (named as the *curvature map*). The level set is allowed to undergo a mean curvature motion. This approximately evolves the medial axis of the level set according to its curvature between the end points and tries to elongate the medial axis at the end points in a tangential direction. The elongated medial axis is taken as the updated position of the curve and the calculations repeated to find the subsequent positions of the curve.

3.1 IDEA OF VISULALIZING AN OPEN CURVE AS A JUNCTION BETWEEN 2 LEVEL-SETS OF CLOSED CURVES

Let Ω be a bounded open subset of $\Re^2$, with $\partial\Omega$ as its boundary. We may visualize an open-ended curve as the common zero level sets of two closed curves. Suppose, we define,

$$\begin{cases} C_1 = \partial\omega_1 = \{(x,y) \in \Omega : \phi_1(x,y) = 0\}, \\ inside(C_1) = \omega_1 = \{(x,y) \in \Omega : \phi_1(x,y) > 0\}, \\ outside(C_1) = \Omega \diagup \omega_1 = \{(x,y) \in \Omega : \phi_1(x,y) < 0\} \end{cases}$$

and,

$$\begin{cases} C_2 = \partial\omega_2 = \{(x,y) \in \Omega : \phi_2(x,y) = 0\}, \\ inside(C_2) = \omega_2 = \{(x,y) \in \Omega : \phi_2(x,y) < 0\}, \\ outside(C_2) = \Omega \diagup \omega_2 = \{(x,y) \in \Omega : \phi_2(x,y) > 0\} \end{cases}$$

(3.1)

where C_1 and C_2 are two closed curves and ϕ_1 and ϕ_2 the corresponding level set functions, and let the open curve $C = C_1 \cap C_2$. In equation (3.1), ω_1 and ω_2 denote two regions in $\Re^2$ and $\partial\omega_1$, $\partial\omega_2$ their corresponding boundaries. We initialize the two closed curves in such a manner that there is a non-zero intersection between their zero level sets, and this intersection is a single connected component that we view as our open-ended curve C.

Now, we initialize C_1 and C_2 such that C_2 encircles the object contour to be tracked. Now, if we evolve both C_1 and C_2 with the evolution equation (2.5), then C_1 and C_2 are guaranteed to have a common intersection that is a singly connected component (i.e., C_1 and C_2 do not cross each other or move away from each other), because their common boundaries have the same curvature as well as image data force components. The evolution stops when the common intersection C of the two curves, which is our open curve, fully tracks the object contour.

This model of evolving the open-ended curve, though numerically easy to implement, is not the implicit evolution of an open curve in the true sense. It requires one of the level sets to completely encircle the contour of the object, which is a serious limitation if the object to be tracked is essentially 1D, or thin filament like in nature without an end. For example, road networks observed from satellite images.

3.2 NEW MODEL: VISUALIZING THE OPEN ENDED CURVE AS A CURVATURE MAP AND EVOLUTION BY A COUPLED DIFFUSION-CONVECTION EQUATION

A new model is proposed below that evolves a *curvature map* (curvature map is defined in section 3.2) of the open-ended curve via diffusion and coupled convection. It visualizes the open-ended curve as the medial axis of the level set of a function defined on the curve (named as the *curvature map*). The level set is allowed to undergo a mean curvature motion. The mean curvature motion approximately evolves the medial axis of the level set according to its curvature between the end points and tries to elongate the medial axis at the end points in a tangential direction. The elongated medial axis is taken as the updated position of the curve and the calculations repeated to find the subsequent positions of the curve. The curve evolution stops when the boundary of the objects to be segmented is detected.

In order to understand some of the mathematical derivations in our new model, we need to understand the concepts of the *Gradient Vector Flow* (GVF) as introduced by Xu and Prince [10].

3.2.1 A BRIEF DISCUSSION ON GRADIENT VECTOR FLOW (GVF) (XU AND PRINCE, 1998 [10])

Suppose we have a potential function f defined over a two dimensional image. A GVF is a vector field $\vec{G}(x,y) = [\bar{u}(x,y), \bar{v}(x,y)]$ defined over the image that minimizes the energy functional

$$E(C) = \iint (\mu(\bar{u}_x^{\,2} + \bar{u}_y^{\,2} + \bar{v}_x^{\,2} + \bar{v}_y^{\,2}) + |\nabla f|^2 |\vec{G} - \nabla f|^2) dx dy \qquad (3.2)$$

The solution $\vec{G}(x,y)$ to equation (3.2) is a vector field that is nearly equal to ∇f when $|\nabla f|$ is large, and is very slowly varying in regions of homogeneous f, i.e., where $|\nabla f|$ is small.

3.2.2 MATHEMATICAL FRAMEWORK OF THE NEW MODEL

In this section we describe the mathematical derivation of the proposed model. The idea is as follows:

- An implicit representation of the open-ended curve called the curvature map is obtained via the calculation of the GVF of the scalar distance function to the open curve. The reader is advised to refer figures 3.1 to 3.4 and figure 3.6 for clear understanding.
- If the curve contains sharp twists and bends, the curvature map may contain bands of high values far away from the position of the open curve that may adversely affect the subsequent calculations. Hence we define a domain function that has a non-zero value only close to the open curve. We then use this domain function to arrive at a modified form of the curvature map that has non-zero values only close to the open curve. Refer to figure 3.5 for clarification.
- With the modified form of the curvature map, we construct a characteristic function for the current position of the open curve, then evolve the boundary of this characteristic function via diffusion and coupled convection for a time period (time period is assumed empirically). The reinitialized boundary of the diffused characteristic function gives a new characteristic function, and the medial axis of the new characteristic function gives the new position of the open curve. Refer figures 3.7 to 3.13 for clarification.
- To find the position of the open curve in the next time instant, we repeat the above-mentioned steps (starting from the curvature map) all over again. The model is now described in an elaborate fashion below.

Let us consider an open-ended curve $C(s):[0,1]\rightarrow \Re^2$, where $C(0)\neq C(1)$. Figure 3.2 shows an open-ended curve. A curvature map for this curve is constructed as follows. Let δ be the scalar distance function to the open curve $C(s)$ (This means, $|\nabla\delta|=1$). Figure 3.3 shows the scalar distance function for the curve in figure 3.2. We evaluate the Gradient Vector Flow (GVF) $\vec{G}$ of this open curve by taking δ as the edge map as in [10]. The GVF field for the distance function in figure 3.3 is shown in figure 3.6. The GVF may be thought of as a smoothed version of the normal gradient field $\nabla\delta$ of δ, so that $\vec{G}$ nearly equals $\nabla\delta$ where $\nabla\delta$ has appreciable magnitude, and is very slowly varying (i.e., abrupt changes in directions are smoothened) in homogeneous regions (i.e., where the value of δ is nearly constant).

We now define a curvature map Ψ as the square of the divergence of this GVF field $\vec{G}$, i.e.,

$$\Psi = (\nabla \circ \vec{G})^2 . \tag{3.3}$$

($\circ$ denotes the vector dot product in the above equation). The curvature map computed from the GVF in figure 3.6 is shown in figure 3.4. To eliminate the effect of bands of high Ψ that are far from the curve, we define a domain function ϕ as,

$$\phi = Ke^{-\left(\frac{\delta}{\sigma}\right)^2} \tag{3.4}$$

and multiply the curvature map with the *Heavyside* function $H(\phi - \varepsilon)$ with $0 < \varepsilon < K$, where K and σ are positive constants. The domain function for the curve in figure 3.2 is shown in figure 3.5. For the open curve $C(s)$, the domain function ϕ over the image domain becomes a bell shaped mound around the curve, and decays exponentially with distance from the curve.

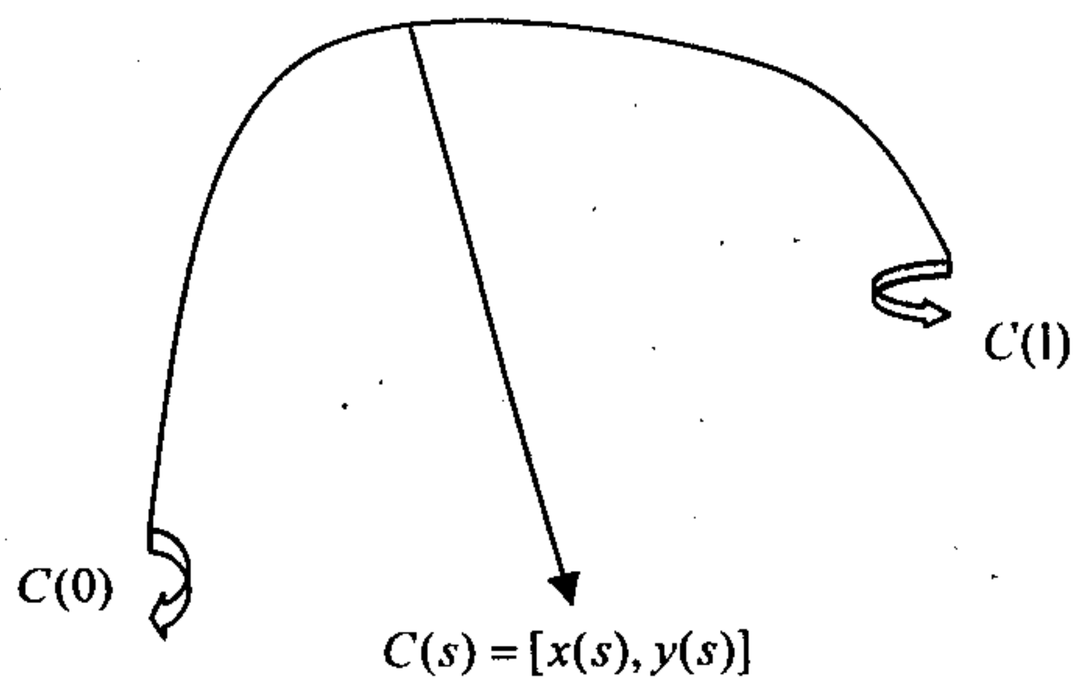

Figure 3.1: The curve $C(s)$, where s or ar- length varies from 0 to 1.

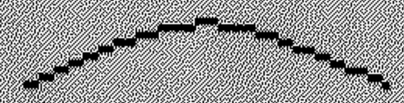

Figure 3.2: An open-ended curve for which we are going to find the curvature map Ψ and domain function ϕ. The size of the image containing the above curve is 100×100.

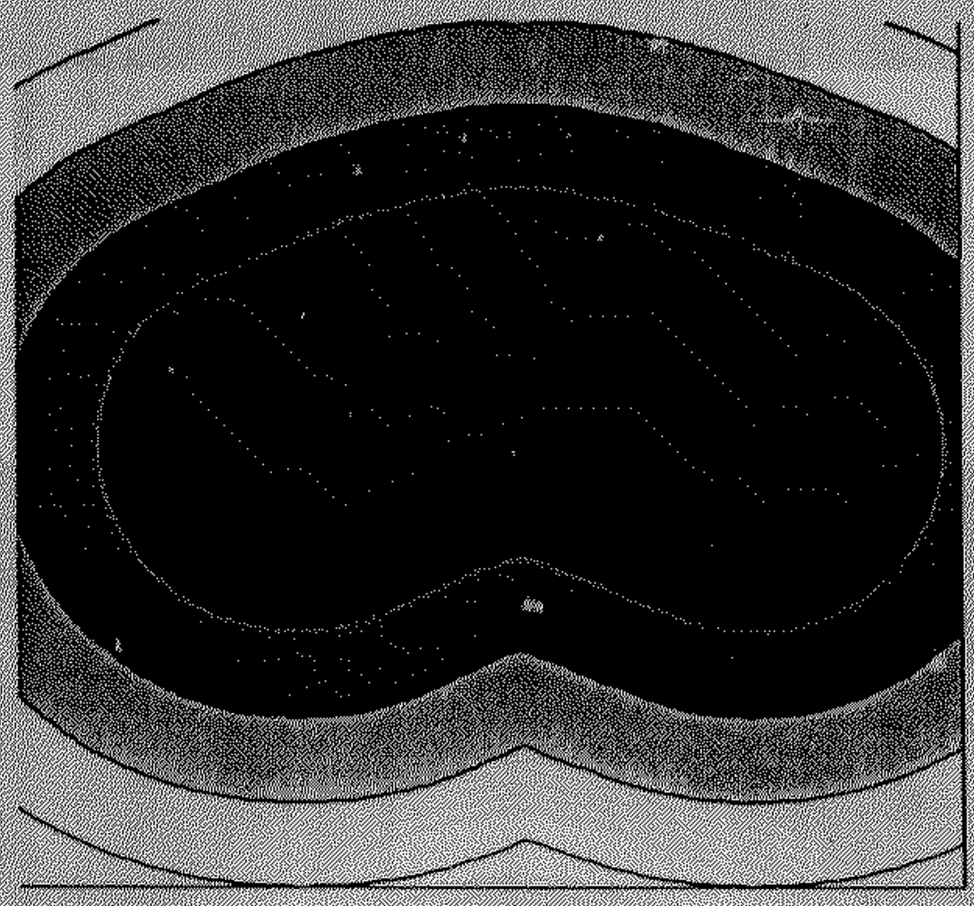

Figure 3.3: The positive scalar distance function to the curve shown in figure 3.2. Color indicates the scalar distance of that point from the curve, a lighter color indicating a greater distance and vice-versa. The scalar distance varies from a value of zero (on the curve points) to a maximum value of fifty (at the boundary of the image).

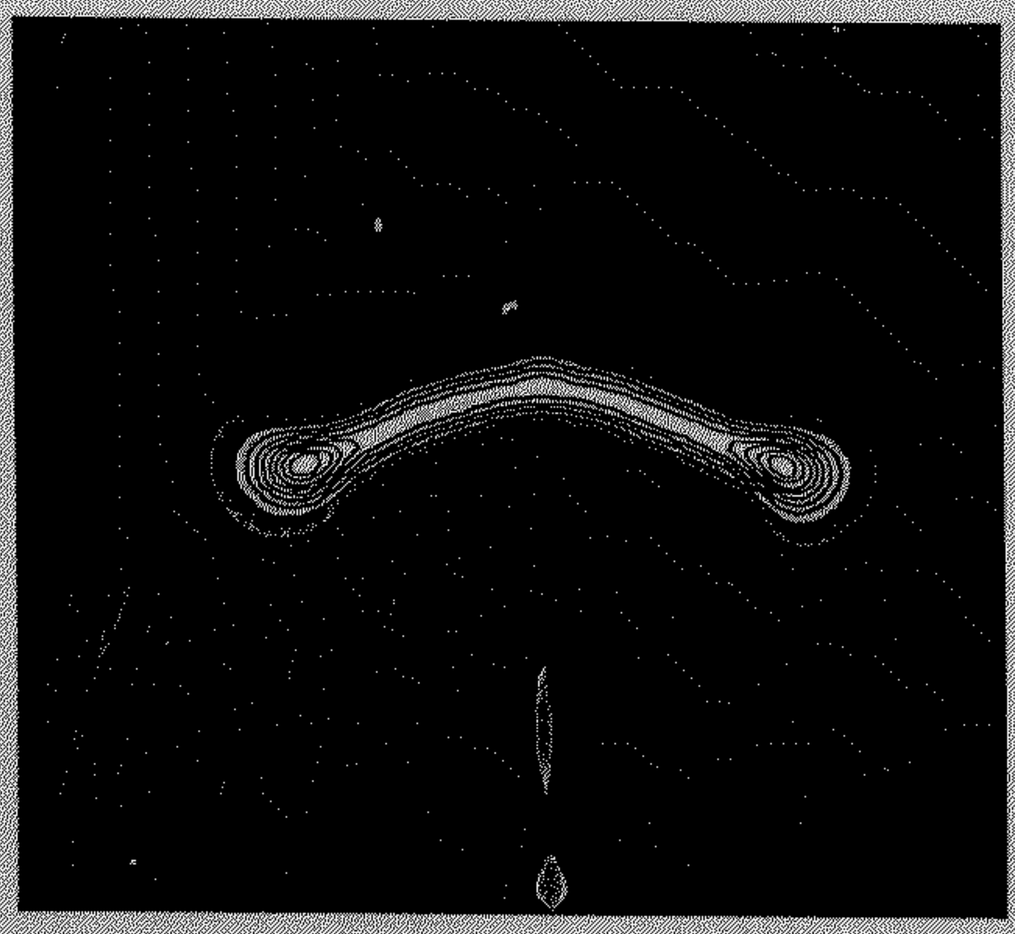

Figure 3.4: The normalized (normalization is done between 0 and 1) curvature map Ψ of the GVF $\vec{G}$ computed from the distance function δ in figure 3.3. Lighter shades indicate values closer to 1, and darker shades indicate values closer to 0.

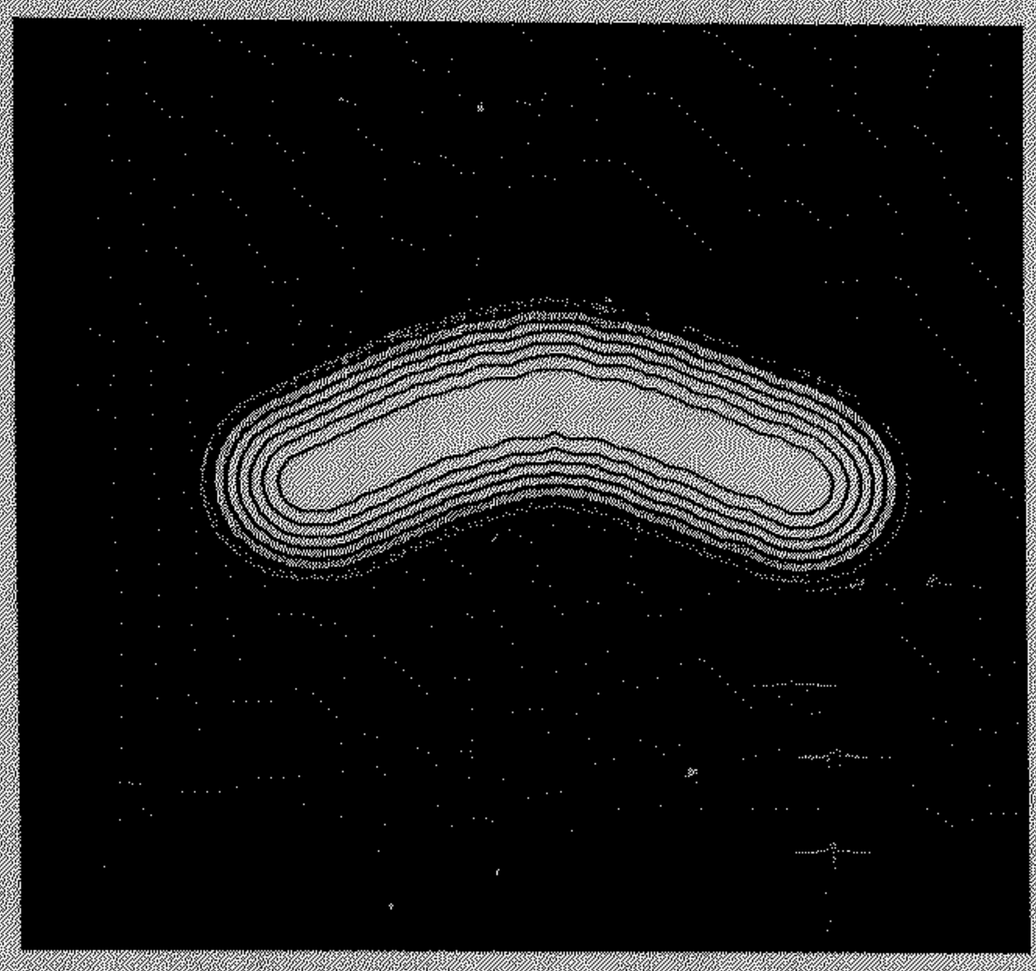

Figure 3.5: The domain function ϕ of the curve in figure 3.2 .The parameters K and σ have the values 10 and 10 respectively. Lighter color indicates a higher value and vice-versa.

As is evident from the figures, the curvature map Ψ forms a narrow band around the position of the curve $C(s)$, with two dumb-bell shaped protrusions at the two end points. This shape can be explained in the following way:

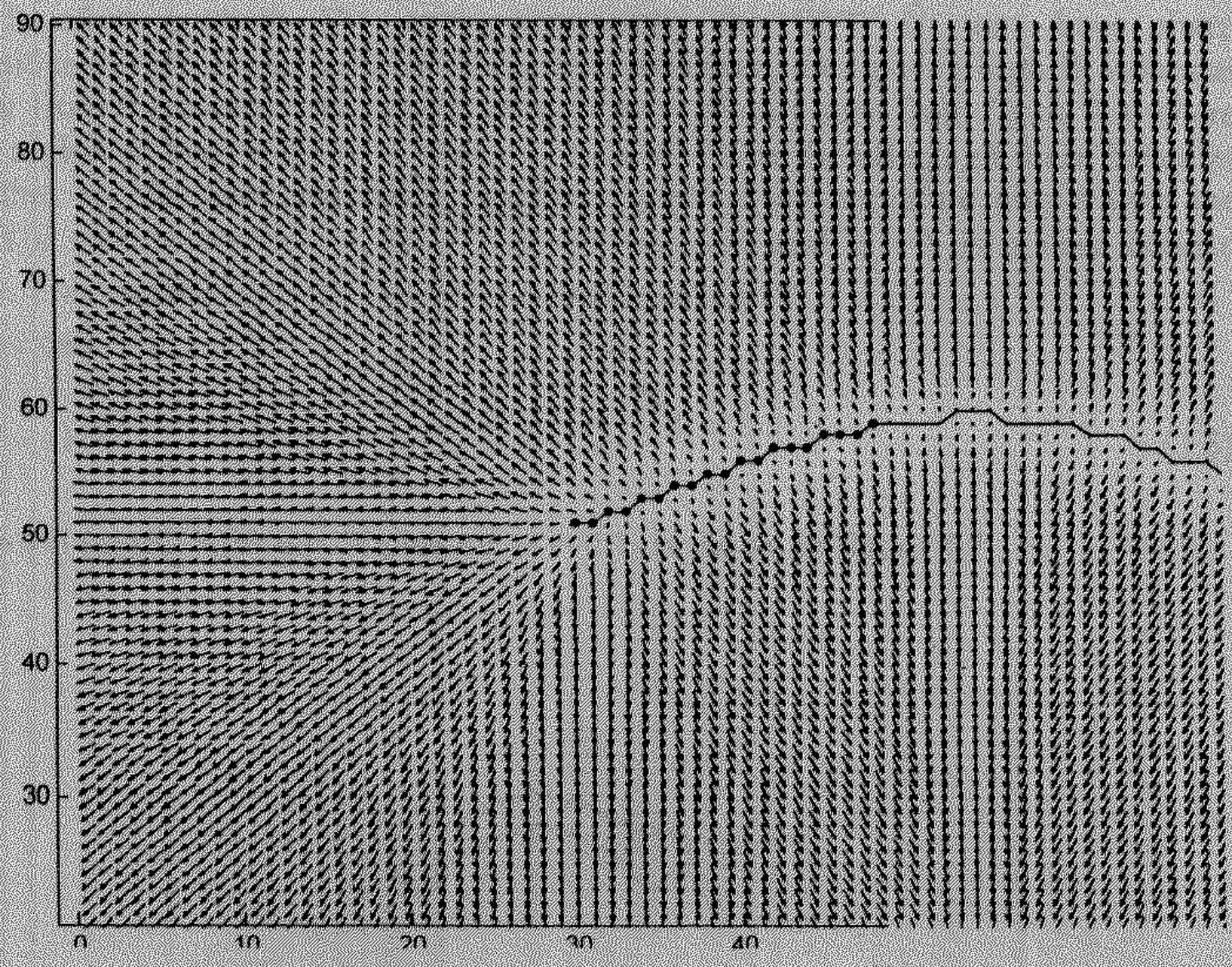

Figure 3.6: The GVF field $\vec{G}$ of the scalar distance function δ in figure 3.3. The left portion of the whole GVF field is magnified and shown in close up in the above figure.

The divergence of the GVF field $\vec{G}$, as seen from figure 3.6, is high in a narrow band along the curve where the vectors have a sudden phase discontinuity and point in opposite directions to each other just along the curve (the phase shift of the vector field is almost 180° here). Also, the divergence is very high at the end points, due to the huge rotation of the vector field about the end points. This rotation in the field propagates quite a distance radially outwards from the end points, which can be clearly seen from figure 3.6. Thus, the square of the divergence of $\vec{G}$, or Ψ, has a high value in a thin band along the curve and a dumb-bell shaped blob at each of the two end points.

From figure 3.5, ϕ decays exponentially as we move out along any normal direction from the curve, and attains values nearly equal to zero within a very short distance from the curve, depending on the parameter σ.

Thus, if we consider a μ-level set[6] of the normalized (where the values have been normalized between 0 and 1) Ψ $(0 < \mu < 1)$, we expect to find a closed curve that has an elongated shape with two dumb-bell shaped protrusions at the ends. We may encounter one possible difficulty here. When the curve is not very smooth or has sharp turns, the distance function gradient $\nabla\delta$ and consequently the GVF $\vec{G}$ may have sharp discontinuities developing at some distance from the curve, thus giving high Ψ values at regions far from the curve. An example of this can be readily seen from figure 3.4 where there is a region of high Ψ far from the curve. To eliminate the effects of these bands of high Ψ s that are far from the curve, we first multiply the curvature map Ψ with the function $H(\phi - \varepsilon)$, where, H is the *Heavyside* function and $\varepsilon > 0$ is a user defined parameter. This cancels the effect of faraway bands of high Ψ.
Thus, if we call $\hat{\Psi}$ as,

$$\hat{\Psi} = H(\phi - \varepsilon) \cdot \Psi \tag{3.5}$$

Then μ-level set of $\hat{\Psi}$ for our Ψ, where $\mu = 0.1$, is shown in figure 3.7.

Figure 3.7: The μ - level set of $\hat{\Psi}$, where $\mu = 0.1$, estimated from the curvature map in figure 3.4 and the domain function in figure 3.5.

We may now note the interesting property of the μ - level set of $\hat{\Psi}$. The middle elongated portion of the level set has low curvature, but the end portions where the dumb bell shaped bulges exist have relatively higher curvature. This can be clearly observed from figure 3.8. Our primary interest is to represent the curve as some function of this level set and then consequently evolve this curve. We represent the curve as the *medial-axis* of μ - level set of $\hat{\Psi}$ (refer figure 3.9 for seeing the medial axis representation).

[6] The μ level set of the function f is defined as the set of points $\{\mathbf{x}\}$ for which $f(\mathbf{x}) = \mu$.

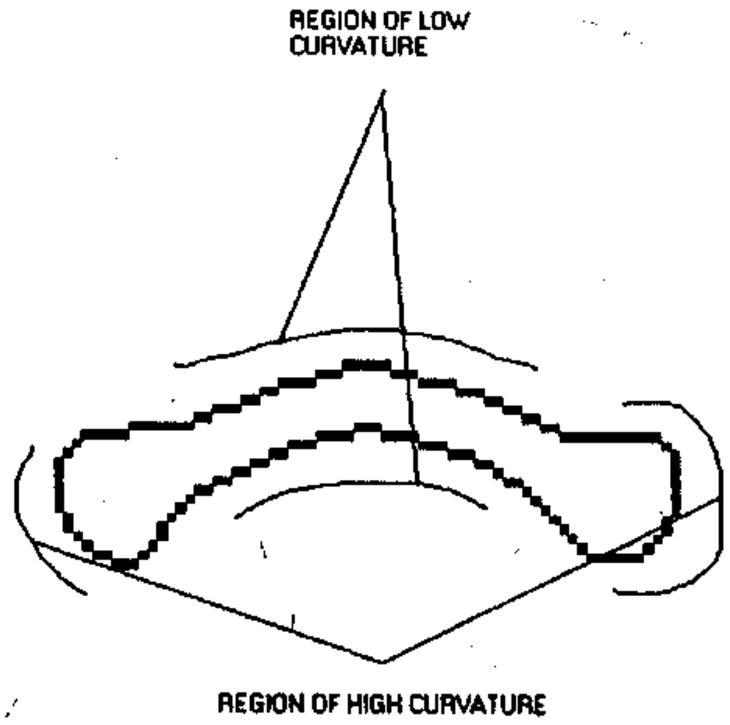

Figure 3.8: Regions of high and low Curvatures along the μ-level set shown in figure 3.7.

Figure 3.9: The medial axis of the level set shown in figure 3.7, shown in bold line, represents the curve.

Now, in order that the curve may grow, we initialize the inside-portion of this μ - level set of $\hat{\Psi}$ with 1 and the outside portion with zero and call it the characteristic function Γ.

$$\Gamma(x,y)=\begin{cases}1 \text{ if } (x,y) \text{ is inside or on the } \mu-\text{leveset of } \hat{\Psi} \\ 0 \text{ otherwise}\end{cases} \tag{3.6}$$

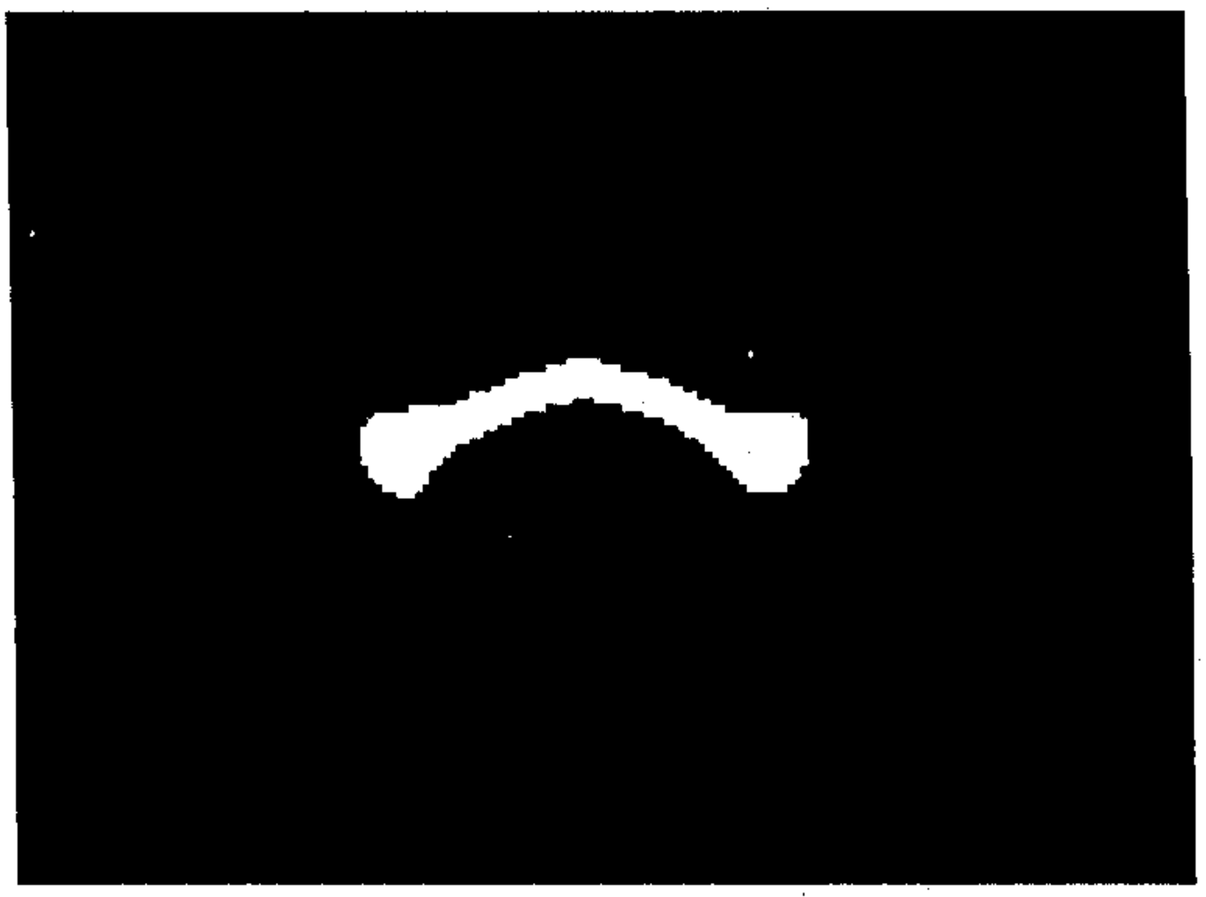

Figure 3.10: Γ for the 0.1 level set shown in figure 3.7. Black represents 0 and white represents 1.

The reader may refer to figure 3.10 to get an understanding of the construction of Γ. Isotropic diffusion with intermediate re-initialization of this function Γ amounts to a mean curvature motion of the boundary of Γ along the normal direction to the boundary (The initial boundary of Γ, we recall, is our μ - level set of $\hat{\Psi}$) that conserves volume [7]. We may recall here that the mean curvature at any point on the boundary of Γ is equal to $\kappa - \kappa_a$, where κ is the curvature at that point, and κ_a is the average curvature evaluated over the whole boundary. Our aim is to somehow elongate the open-ended curve, and we note that, evolving the boundary of Γ according to its mean curvature would fatten out the regions of low curvature of the μ - level set (this region is along the middle of the level set as shown in figure 3.8) but would restrict bulging or growing out of the dumb-bell shaped ends that had a high curvature. This, in turn, would mean that this unequal movement of the boundaries will ultimately smooth out the boundary of Γ, the bulges at the end would disappear and the boundary will grow outwards. The new boundary, since it has a uniform band like elongated structure, would have a new *medial axis*, which will be elongated at the ends compared to the previous curve, in a direction roughly parallel to the tangents at the ends of the original curve.

Therefore, let us state the equation of updation for Γ.

$$\frac{\partial \Gamma}{\partial t} = \nabla^2 \Gamma \tag{3.7}$$

We apply equation (3.7) for a time period T, and then reinitialize the boundary of Γ in the following way –

$$\Gamma_{\text{re-initialized}} = \begin{cases} 1 & \text{if} \quad \Gamma_{\text{previous}} \geq \lambda \\ 0 & \text{otherwise} \end{cases} \tag{3.8}$$

Here, again, $0 < \lambda < 1$ is a user-defined threshold.

As noted in [7], diffusion generated motion as in equation (3.7) (which is equivalent to evolving the boundary of the region in its normal direction with speed equal to the mean curvature), can be realized by convolving the region Γ with a Gaussian Kernel, with width equal to $\sqrt{T}$, where T is the time period for diffusion. The effect of this diffusion with the Gaussian kernel is shown in figure 3.11.

Thus, we may do the same task as equations (3.7) and (3.8) with the help of the single equation –

$$\Gamma_{re-initialized} = \begin{cases} 1 & if \quad \Gamma_{previous} * \mathrm{K} \geq \lambda \\ 0 & otherwise \end{cases} \tag{3.9}$$

where, K is a Gaussian kernel with width $\sqrt{T}$, and $*$ denotes convolution.

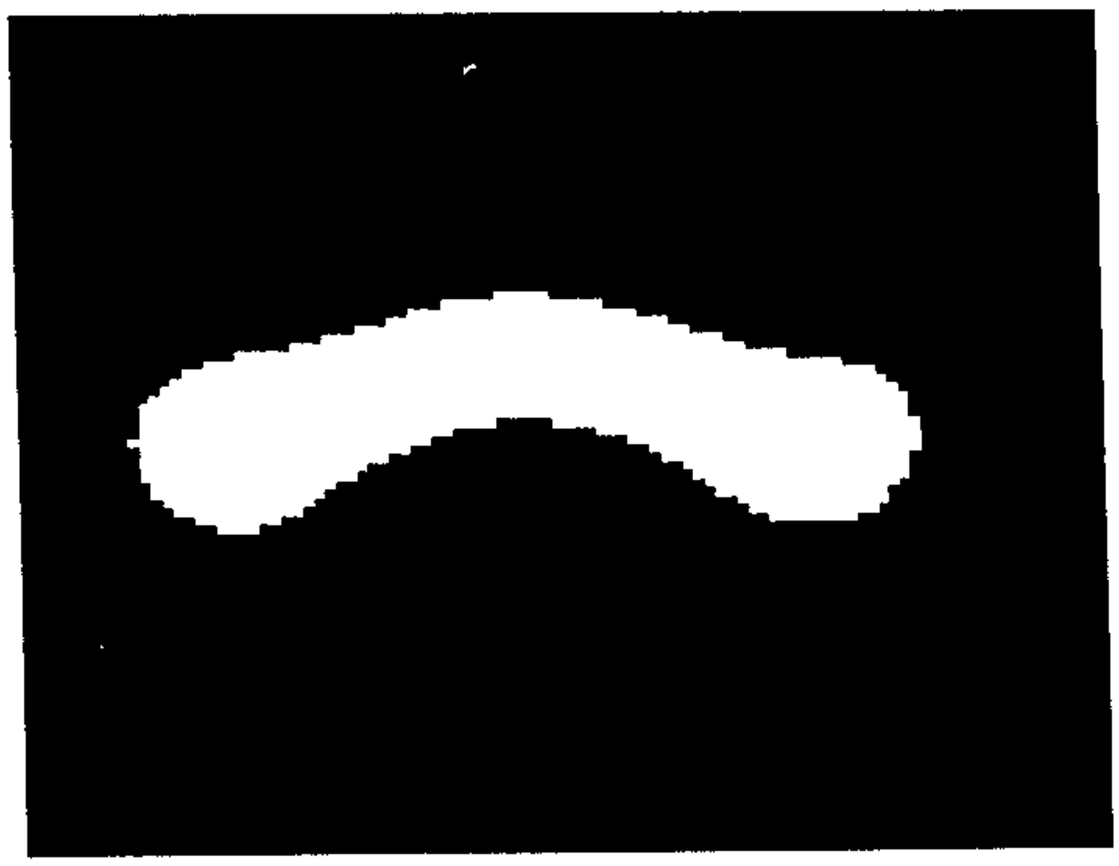

Figure 3.11: Updated Γ after convolving Γ in figure 3.10 with a Gaussian kernel of width 4.

Figure 3.12: The new boundary of the updated Γ in figure 3.11.

Figure 3.13: The new medial axis of the updated boundary in figure 3.12 that is slightly elongated compared to the previous curve in figures 3.2 and 3.9 at the ends.

In case the evolution is aided by any external force field $\vec{F}$ guiding the evolving curve towards an object boundary, $\vec{F}$ is interpreted as a velocity field that transports the characteristic function Γ along with $\vec{F}$. The equation (3.7) is modified to the familiar diffusion-convection equation for concentration transport (Γ is interpreted now as a concentration profile) as

$$\frac{\partial \Gamma}{\partial t} = \nabla^2 \Gamma - \eta \nabla \circ (\Gamma \vec{F}) . \tag{3.10}$$

$\eta \geq 0$ controls the relative weight of the convection term. Or, using the Gaussian convolution approach of equation (3.9),

$$\Gamma_{re-initialized} = \begin{cases} 1 & if \quad \Gamma_{previous} * \mathrm{K} - \eta \nabla \circ (\Gamma_{previous} \vec{F}) \geq \lambda \\ 0 & otherwise \end{cases} \tag{3.11}$$

Obviously, using equation (3.11) means that the time period T used in evaluating the width of the Gaussian kernel should be much smaller compared to T in equation (3.9). This is because, the aim of equation (3.10) is convection along with diffusion, and a smaller T means diffusing Γ simultaneously with convection is better modeled by a smaller time step. Choosing higher time steps mean effectively separating out the diffusion and convection processes in time. We summarize our algorithm in the next section.

3.2.3 ALGORITHM EVOLVE_OPENCURVE

As long as curve $C(s)$ does not capture the full object contour, continue:

1) Take the Curve $C(s)$, calculate its modified curvature map $\hat{\Psi}$ using equations (3.3), (3.4), (3.5), and choosing a suitable ε.
2) Choose a suitable μ, and calculate the μ-level set of $\hat{\Psi}$. Then construct Γ using equation (3.6).
3) Update Γ using equation (3.11) choosing a suitable time step T. Construct the medial axis of this updated Γ through morphological thinning of the new Γ. Take this medial axis as the new curve $C(s)$ and return to step 1 if the curve has not fully tracked any contour (or any other objective criteria has been met).

We can modify the convective diffusive model presented in equations (3.10) and (3.11) to specially suit the segmentation of one-dimensional filament like structures in 2D images.

We may assume that the one-dimensional structures have an average intensity that is in contrast (i.e., considerably different) from the average intensity of the background. Hence, we define a coefficient called the *coefficient of intensity difference* ℓ defined at every position (x,y) of the image I as

$$\ell(x,y) = \frac{1}{0.1 + \left| I_p(x,y) - \frac{\iint_{(x,y)\in I} \Gamma I_p(x,y)\,dx\,dy}{\iint_{(x,y)\in I} \Gamma\,dx\,dy} \right|}. \tag{3.12}$$

I_p denotes the intensity value of the graylevel image I. It can be observed from equation (3.12) that ℓ takes a higher value when the intensity (or color) value of the point (x,y) becomes very close to the average intensity value inside the characteristic function Γ, and vice-versa.

We also define the very familiar *anisotropic diffusion coefficient* $\wp$ defined at every point over the same image I as

$$\wp(x,y) = \frac{1}{0.1 + |\nabla I_p(x,y)|}. \tag{3.13}$$

A modified form of the equation (3.11) can be thus defined as

$$\Gamma_{re-initialized} = \begin{cases} 1 \; if \; \wp\ell(\Gamma * K) \geq \lambda \\ 0 \; otherwise \end{cases} \tag{3.14}$$

where the Gaussian kernel has the width approximately equal to $\sqrt{T}$, where T is the time period of an equivalent isotropic diffusion as stated in equation (3.9). Equation (3.14) is designed keeping the following logic in mind. If we initialize an open-ended curve inside a 1D filament like structure, the characteristic function Γ (of the open-ended curve) obtained from equation (3.6) undergoes an isotropic diffusion by convolving it with the Gaussian kernel K. The product term $\wp\ell$ takes a very low value at the edges of the filament (since $\wp$ is low here) as well as areas that are just outside the boundary of the filament (ℓ is low here due to high intensity difference between the average intensity inside Γ and the intensity of the area just outside the boundary of Γ). Hence, pre-multiplying the diffused Γ with $\wp\ell$ negates the effects of the diffusion in areas that are just at the edges or just outside the boundary of the filament. Thus the re-initialized Γ tries to stay inside the filament that we are attempting to segment.

3.2.4 DISCUSSION ON THE GEOMETRY OF EVOLUTION OF THE CURVE

The familiar diffusion-convection equation generally used in the transport phenomena of concentration profile (in the fields of mass transport, heat transport, etc) is thus effectively applied to evolve the open curve. Following is an explanation of the internal mechanics of the new process that makes it work, and also try to categorize the geometric deformation undergone by the evolving curve.

In the case where no external force field from the image data exists, we are left with equation (3.7). It is the simple isotropic diffusion equation which evolves the boundary of Γ according to its mean curvature [7], while preserving its volume. Hence, we may expect the boundary to flatten out its high curvature regions and approach the shape of a circle in the limit. Consequently, the medial axis of Γ is expected to undergo a curvature driven motion, and in the limit, it should vanish to a point. So why does the open curve elongate ?

Notice that, when we initialize the set Γ, which has dumb-bell shaped boundaries towards the ends, its medial axis has roughly the length of the old curve. The diffusion process in the early stage tries to flatten out the dumb-bell shaped portions to a uniform thickness as the rest of the boundary, all the while pushing the boundary of Γ outwards. Thus, as the dumb-bells flatten out and grow outwards, the end points of the medial axis of the evolving Γ gradually moves outwards towards the centre of the ever-flattening dumb-bells till the boundary of Γ achieves considerable smoothness. It is after this stage that Γ tries to evolve towards a circle, and a choice of an appropriate λ in equation (3.8) restricts further evolution of the boundary of Γ, finds out the elongated medial axis and re-initializes the curve $C(s)$. Thus, the elongation at the end points is expected to occur in an outward tangential direction, while between the end points, the medial axis is expected to undergo a curvature driven deformation that tries to straighten it out.

When a force term $\vec{F}$ is present to guide the evolution, the growth of the boundary is expected to be towards the direction of $\vec{F}$. Thus the set Γ, while flattening out at the end portions, moves *bodily* towards the object contour directed to by $\vec{F}$. Thus the medial axis undergoes elongation at the end points while moving and conforming to the object boundary.

The logic behind equation (3.14) has already been described after it had been defined, and is expected to give a similar result as equation (3.11).

3.2.5 NUMERICAL IMPLEMENTATION OF THE MODEL

We treat the variables in equation (3.10) as functions of Cartesian space coordinates x, y and time t. Thus, equation (3.10) is re-written as

$$\frac{\partial \Gamma(x,y,t)}{\partial t} = \nabla^2 \Gamma(x,y,t) - \eta \nabla \circ (\Gamma(x,y,t)\vec{F}(x,y)) \tag{3.15}$$

To set up the iterative solution in our rectangular grid, let the indices i, j and n correspond to x, y, and t respectively, and let the spacing between the pixels be Δx and Δy and the time step for each iteration be Δt. Then the required partial derivatives can be evaluated as

$$\frac{\partial \Gamma(x,y,t)}{\partial t} = \frac{1}{\Delta t}(\Gamma_{i,j}^{n+1} - \Gamma_{i,j}^{n})$$

$$\nabla^2 \Gamma(x,y,t) = \frac{1}{\Delta x \Delta y}(\Gamma_{i+1,j}^{n} + \Gamma_{i,j+1}^{n} + \Gamma_{i-1,j}^{n} + \Gamma_{i,j-1}^{n} - 4\Gamma_{i,j}^{n})$$

$$\nabla \circ (\Gamma(x,y,t)\vec{F}(x,y)) = (\frac{\vec{F}(x)_{i+1,j}\Gamma^n_{i+1,j} - \vec{F}(x)_{i-1,j}\Gamma^n_{i-1,j}}{2\Delta x}) + (\frac{\vec{F}(y)_{i,j+1}\Gamma^n_{i,j+1} - \vec{F}(y)_{i,j-1}\Gamma^n_{i,j-1}}{2\Delta y})$$

$\vec{F}(x)_{i,j}$ and $\vec{F}(y)_{i,j}$ denote the x and y component of the vector field $\vec{F}$ respectively.

Thus the finite difference form of the iterative solution to (3.15) arrives at

$$\Gamma^{n+1}_{i,j} = (\frac{\Delta t}{\Delta x \Delta y} + \frac{\eta\vec{F}(x)_{i+1,j}}{2\Delta x})\Gamma^n_{i+1,j} + (\frac{\Delta t}{\Delta x \Delta y} - \frac{\eta\vec{F}(x)_{i-1,j}}{2\Delta x})\Gamma^n_{i-1,j}$$
$$+ (\frac{\Delta t}{\Delta x \Delta y} + \frac{\eta\vec{F}(y)_{i,j+1}}{2\Delta y})\Gamma^n_{i,j+1} + (\frac{\Delta t}{\Delta x \Delta y} - \frac{\eta\vec{F}(y)_{i,j-1}}{2\Delta x})\Gamma^n_{i,j-1} + (1 - \frac{4\Delta t}{\Delta x \Delta y})\Gamma^n_{i,j} \quad (3.16)$$

The finite difference form of equation (3.14) can be similarly stated as:

$$\ell_{i,j} = \frac{1}{0.1 + |I_{p_{i,j}} - \frac{\sum_{(i,j)\in I}\Gamma_{i,j}I_{p_{i,j}}}{\sum_{(i,j)\in I}\Gamma_{i,j}}|}. \quad (3.17)$$

$$\wp_{i,j} = \frac{1}{0.1 + \sqrt{(\frac{I_{p_{i+1,j}} - I_{p_{i-1,j}}}{2\Delta x})^2 + (\frac{I_{p_{i,j+1}} - I_{p_{i,j-1}}}{2\Delta y})^2}}. \quad (3.18)$$

$$\Gamma^{n+1}{}_{i,j} = \wp_{i,j}\ell_{i,j}(\Gamma^n_{i,j}\Theta K). \quad (3.19)$$

Θ is used for denoting the discrete convolution in equation (3.19).We implement equations (3.16) and (3.19) on various initial open-ended curves in various synthetic and real images are summarized in the next chapter (the success and the failure stories).

4. RESULTS AND DISCUSSIONS

We present some results of applying the new model of implicit evolution of open-ended curves to some synthetic and real images. Some of these images exhibit one-dimensional filament like structures that are nearly impossible to segment with traditional closed contour models. Each of these images have been treated to remove noise or sharpen the edges of the objects of interest, specific details of which will be discussed while presenting the specific examples.

4.1 DETECTING A SYNTHETIC ELLIPSE WITH THE MODEL IN SECTION 3.1

We have applied equation (3.1) in evolving an open-ended curve to capture the contour of a synthetic ellipse in a 200×200 image. The two closed curves C_1 and C_2 described in equation (3.1) are taken as two rectangles. C_2 completely encircles the ellipse before the iterations begin. The level sets of the two closed curves C_1 and C_2 undergo curvature driven motion with a stopping function (that has the form of the edge-detector in equation (3.13)) following equation (2.5). The initial position of the intersection of the level sets of C_1 and C_2, which is our open curve C, is shown in red at iteration 1. The open curve evolves according to equation (3.1) and equation (2.5) and captures the contour of the ellipse completely. The position of the open curve at iterations 1, 2, 40 and 60 are shown in figures 3.14(a)-3.14(d).

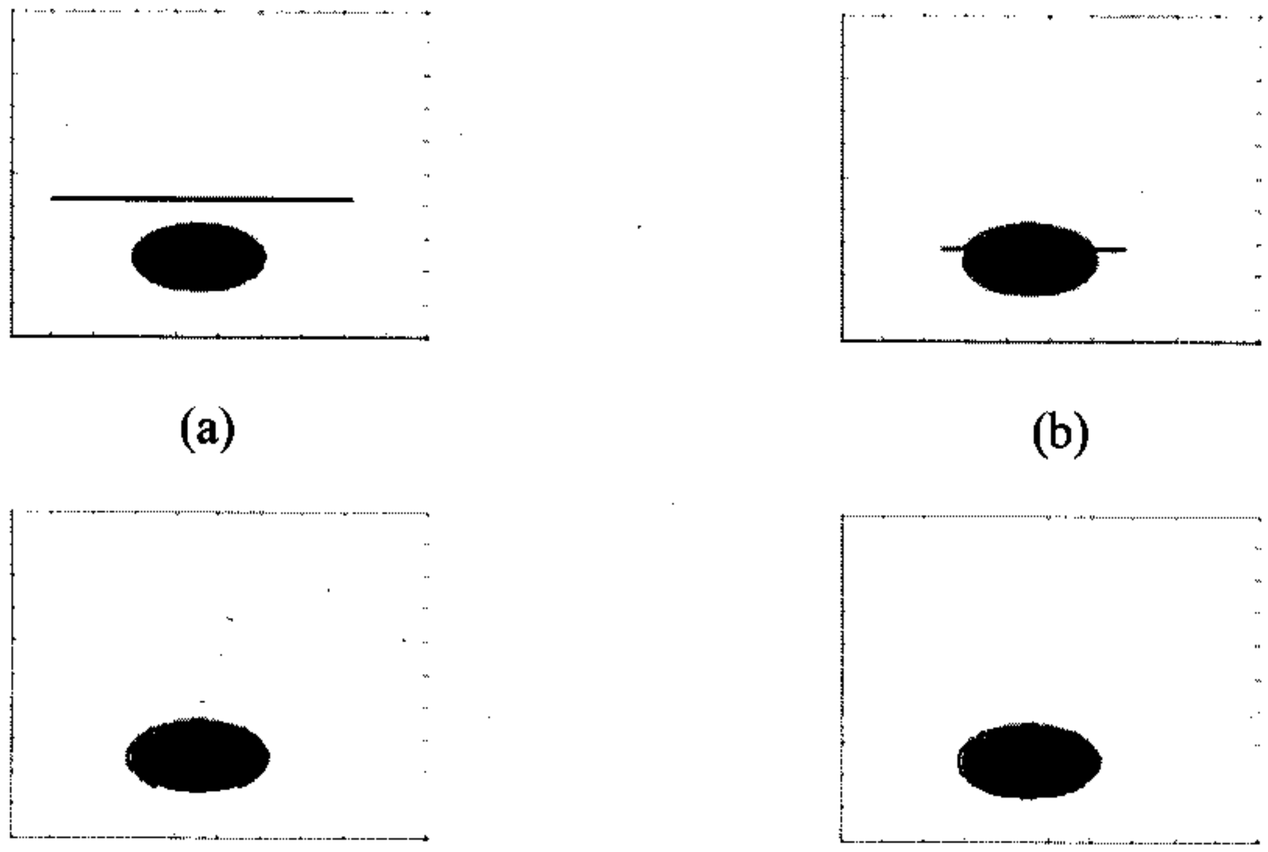

Figure 3.14: Result of applying equation (3.1) to a synthetic 200×200 image of an ellipse in black. (a) The red curve denotes the position of the open curve at iteration 1. (b) The curve at iteration 20. (c) The curve at iteration 40. (d) The curve has converged at iteration 60.

4.2 DETECTING THE CONTOUR OF A TABLE TENNIS BAT IN A REAL IMAGE WITH THE MODEL IN SECTION 3.1

Again, we have applied equation (3.1) in evolving an open-ended curve to capture the contour of a real image of a table tennis bat in a 343×435 *image*. Arrangement of C_1 and C_2 is similar to that in example 4.1. The open curve C, shown in red in figure 3.15(a) denotes the initial position. Figures 3.15(b), 3.15(c) and 3.15(d) show the position of the curve at iterations 10, 20, and 30. The open curve completely detects and captures the contour of the table tennis bat.

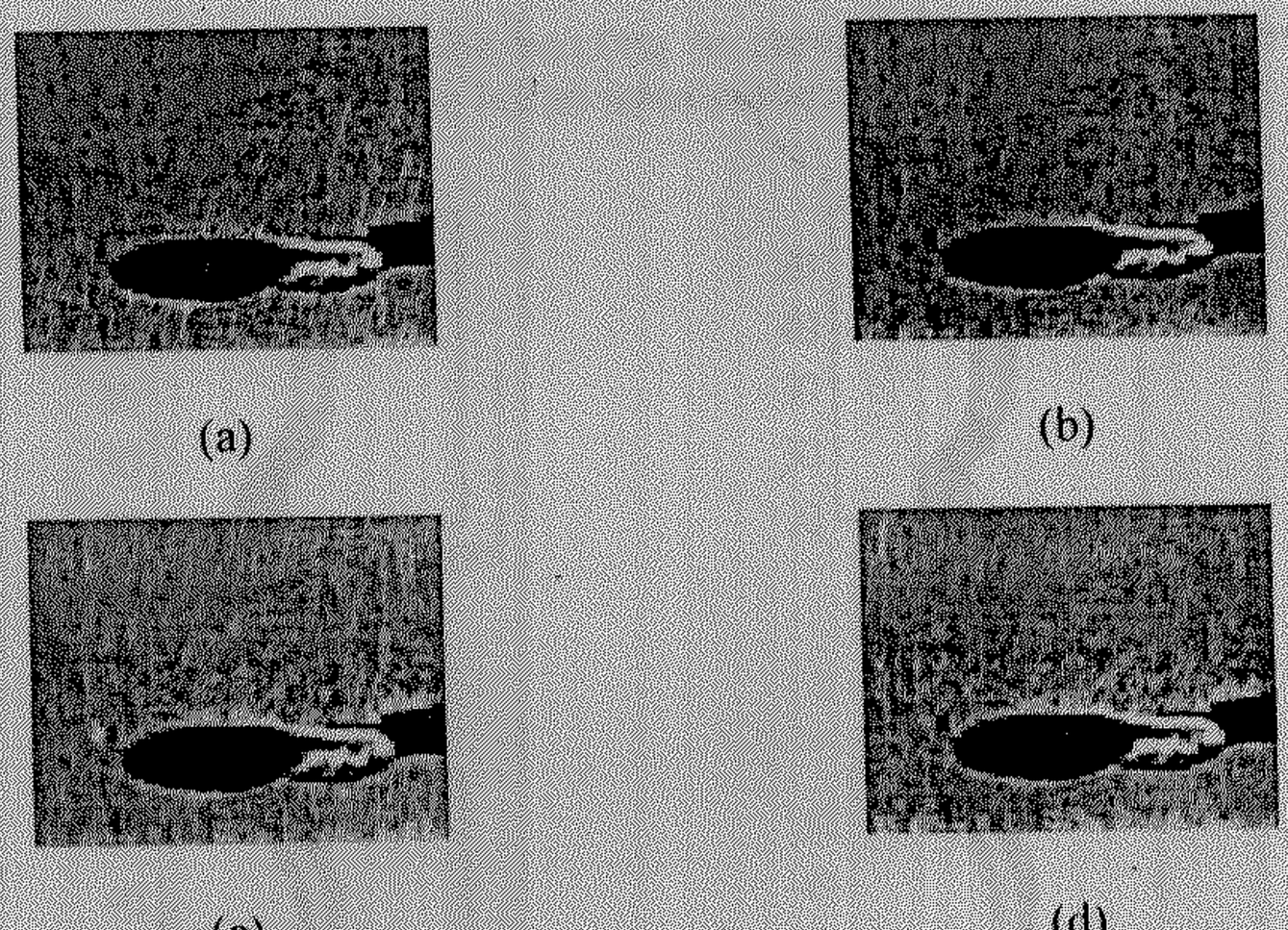

Figure 3.15: Result of applying equation (3.1) to a 343×435 real image of a table tennis bat. The red curve denotes the position of the open curve. (a) The curve at iteration 1. (b) The curve at iteration 10. (c) The curve at iteration 20. (d) The curve has fully captured the contour of the bat at iteration no 30.

4.3 DETECTING A SYNTHETIC ROAD MAP WITH THE MODEL IN SECTION 3.2

We have applied equation (3.14) in evolving an open-ended curve to segment and approximate the shape of a synthetic 100×100 image of a black road against a white background. The time spacing Δt, and λ, has been taken as 0.001 and 4 respectively in equation (3.14) for calculations. The width of the Gaussian kernel is taken as 4. The synthetic image has been blurred using a Gaussian kernel of width 1, and then the coefficient $\wp$ calculated from equation (3.13). An open curve is initialized within the road before the start of calculations. Figures 3.16(a), 3.16(b), 3.16(c), and 3.16(d) denote the open curve positions at red iteration 1, 2, 4 and 6 respectively.

Notice that the curve can follow the bending or curvature of the road even though an almost linear structure is used as the initial open curve.

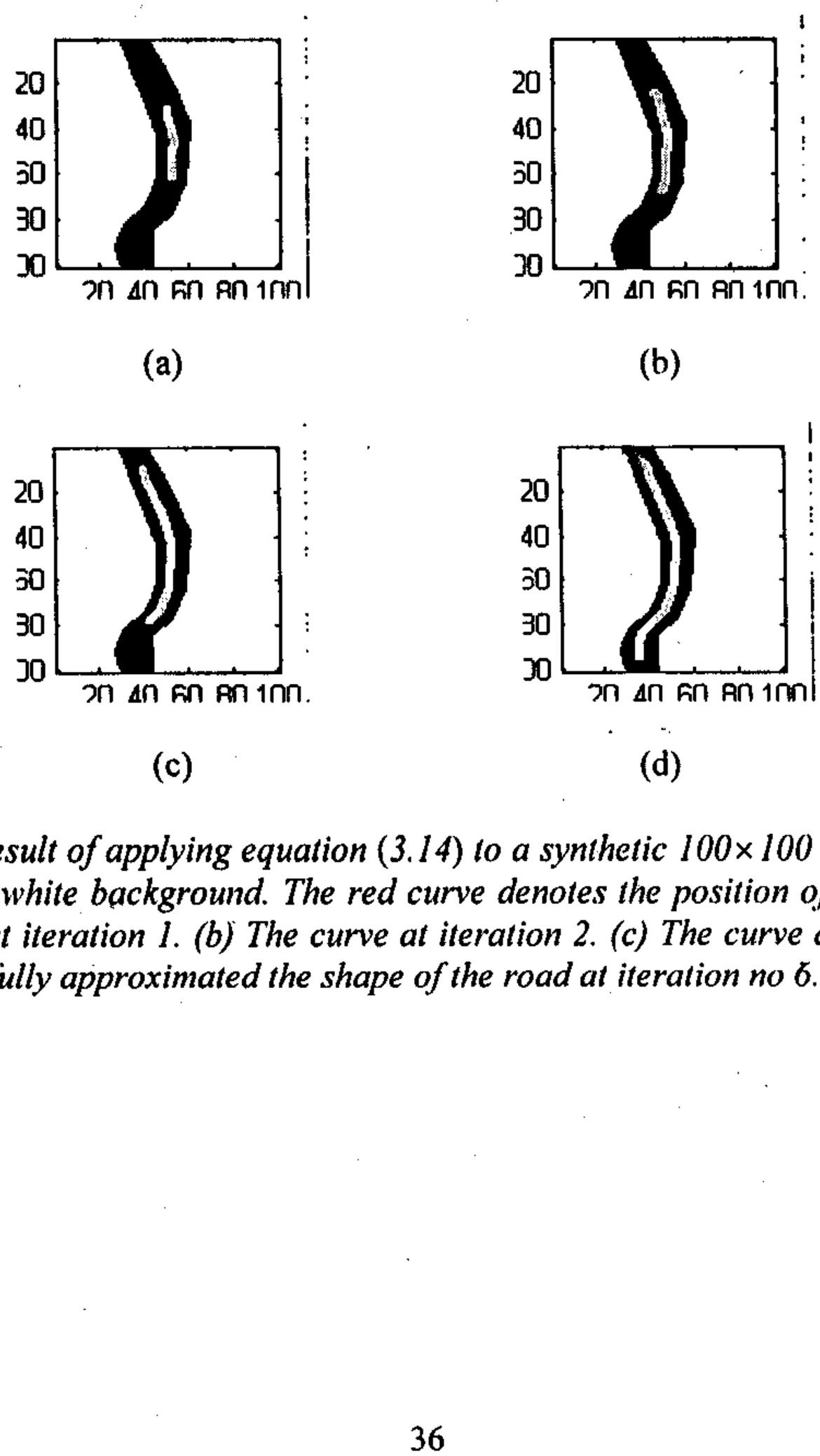

Figure 3.16: Result of applying equation (3.14) to a synthetic 100×100 image of a black road against a white background. The red curve denotes the position of the open curve. (a) The curve at iteration 1. (b) The curve at iteration 2. (c) The curve at iteration 4. (d) The curve has fully approximated the shape of the road at iteration no 6.

4.4 DETECTING ANOTHER SYNTHETIC ROAD MAP WITH THE MODEL IN SECTION 3.2

We have applied equation (3.14) in evolving an open-ended curve to segment and approximate the shape of a synthetic 100×100 image of a black road against a white background. The road divides into two parts at the middle. The parameters for the model are same as that in example 4.3. The open curve is initialized in red at the center of the road. Figures 3.17 (a)-(d) show the position of the open curve at iterations 1, 3, 7 and 14 respectively.

A very interesting property of the model in equation (3.14) can be noted from the following figures. The open curve divides into two parts and follows the two separate branches of the road (as can be seen from figures 3.17(b) and 3.17(c)). Thus, the proposed model in equation (3.14) is *topology-adaptive*, i.e., it can capture and adapt to complex shapes of filaments like forks (as in figure 3.17) and Y junctions. It is thus possible to segment topologically complex filament networks with a little bit of adaptation of the model in equation (3.14).

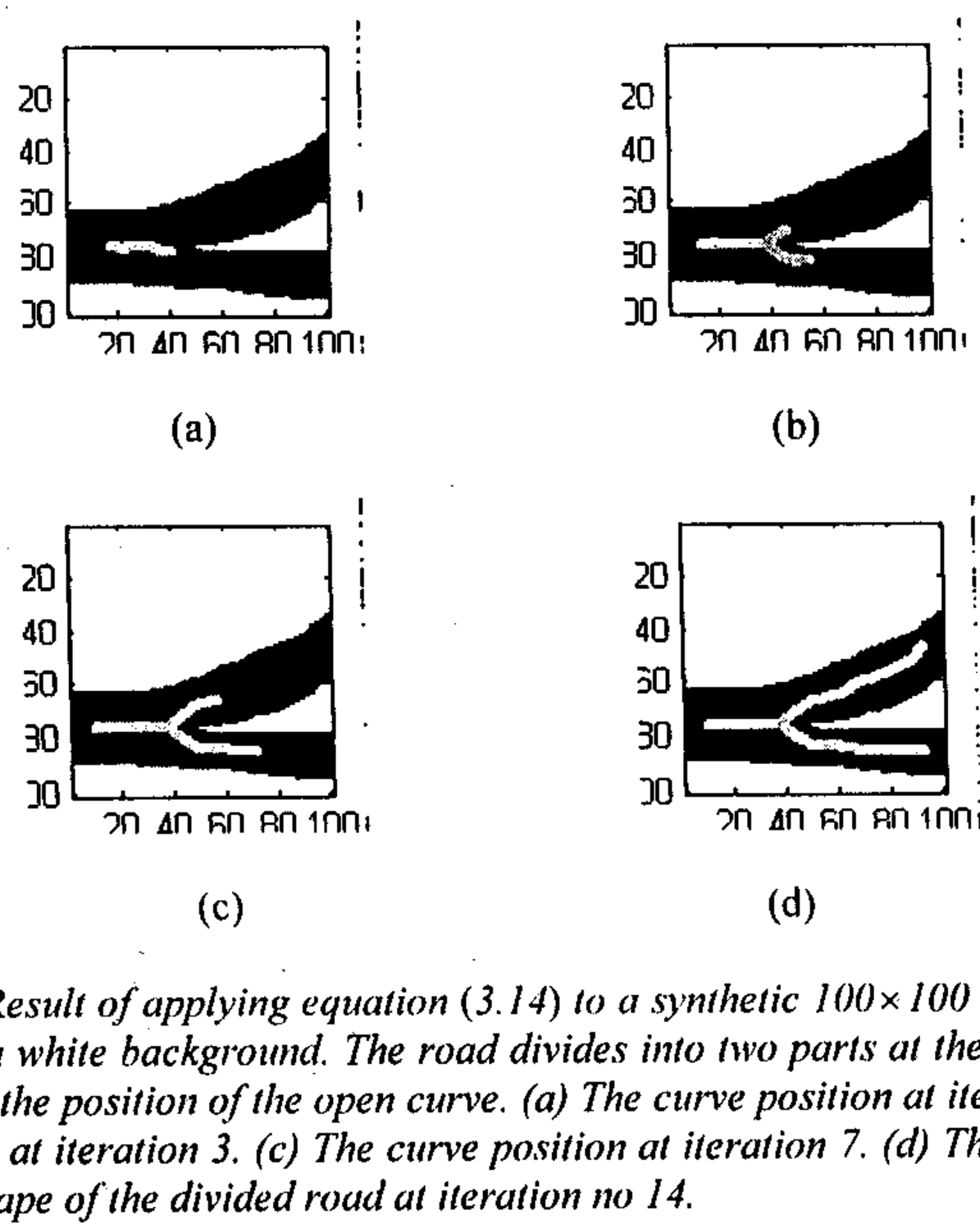

Figure 3.17: Result of applying equation (3.14) to a synthetic 100×100 image of a black road against a white background. The road divides into two parts at the middle. The red curve denotes the position of the open curve. (a) The curve position at iteration 1. (b) The curve position at iteration 3. (c) The curve position at iteration 7. (d) The curve has fully tracked the shape of the divided road at iteration no 14.

EXAMPLE 4.5 DETECTING A SYNTHETIC CIRCLE WITH THE MODEL IN SECTION 3.2

We have applied equation (3.10) in evolving an open-ended curve to approximate the shape of a synthetic 100×100 image of a green circle against a white background. The value of Δt, λ, T and η has been taken as 0.001, 0.25, 0.04 and 1 for calculations. The open curve is initialized in red. Figures 3.18(a)-(d) show the positions of the open curve at iterations 1, 4, 10 and 16 respectively.

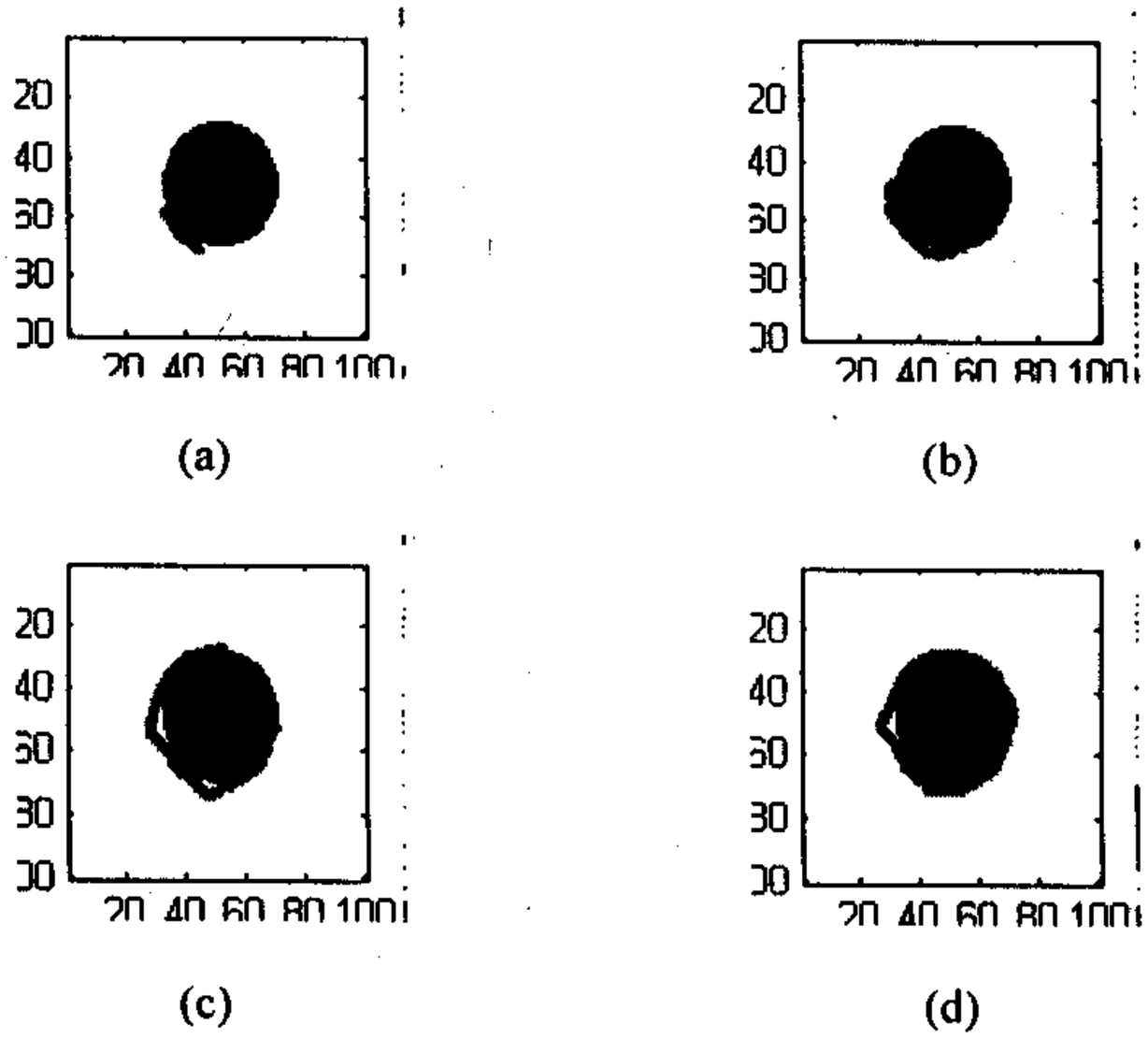

Figure 3.18: Result of applying equation (3.10) to a synthetic 100×100 image of a green circle against a white background. The red curve denotes the position of the open curve. (a) The curve at iteration 1. (b) The curve at iteration 4. (c) The curve at iteration 10. (d) The curve has captured the shape of the circle at iteration no 16.

4.6 DETECTING A ROAD FROM A REAL SATELLITE IMAGE WITH THE MODEL IN SECTION 3.2

We have applied equation (3.10) in evolving an open-ended curve to approximate the shape of a synthetic 128×124 image of a real 128×124 image of a satellite picture of a road. The road is identifiable as the thin black line along the center. The values of the parameters are same as in example 4.5. Figures 3.19(a)-(d) show the positions of the open curve at yellow through iterations 1, 5, 13 and 20 respectively.

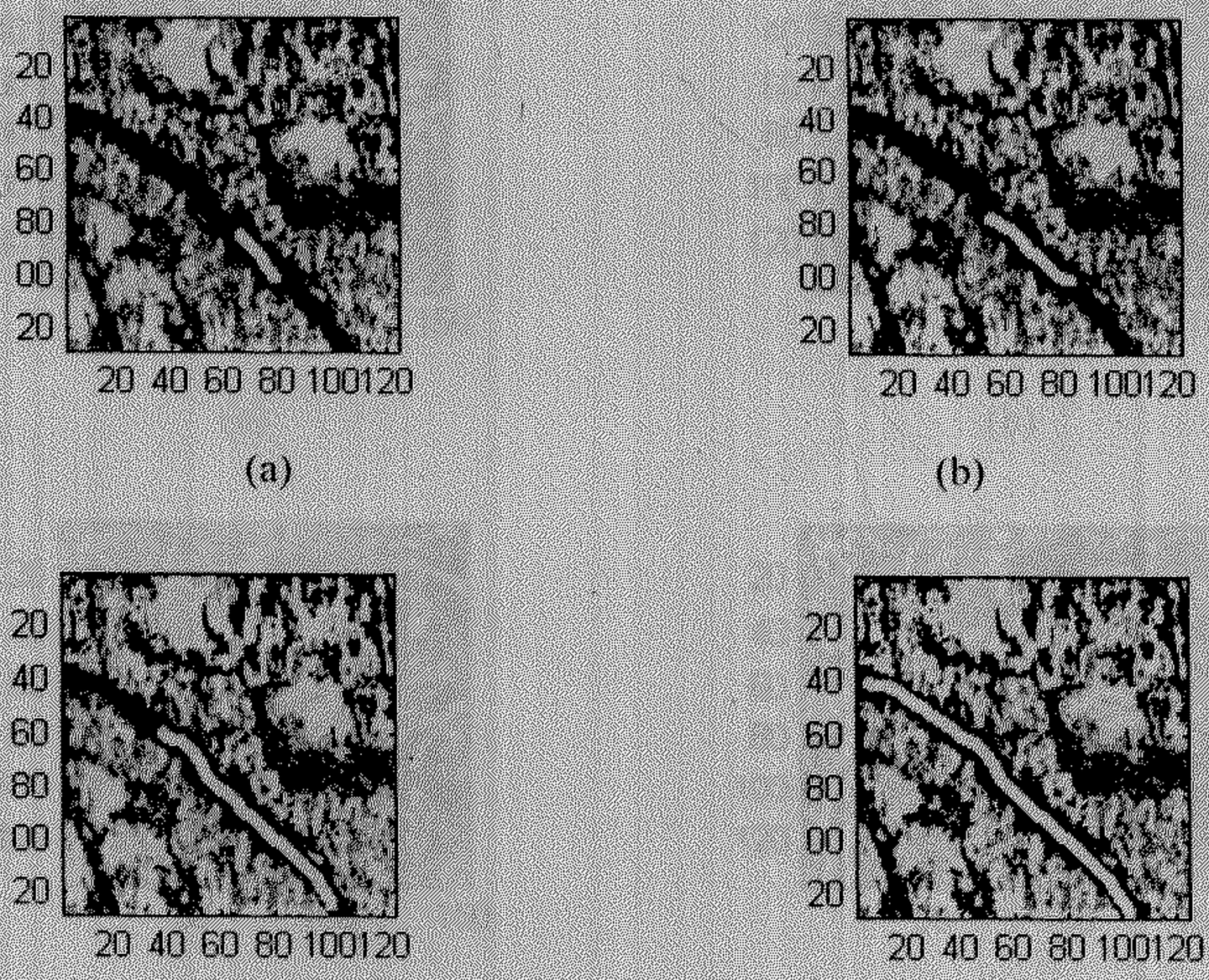

Figure 3.19: Result of applying equation (3.10) to a real 128×124 satellite picture of a road. The road is identifiable as the thin black line along the center. The yellow curve denotes the position of the open curve. (a) The curve at iteration 1. (b) The curve at iteration 5. (c) The curve at iteration 13. (d) The curve has converged at iteration 20.

4.7 DETECTING A RIVER FROM A REAL SATELLITE IMAGE WITH THE MODEL IN SECTION 3.2

We have applied equation (3.14) in evolving a real 138×152 image of a satellite picture of a river. The river is identifiable as the thin black curve along the center. Parameter values are same as in example 4.3. Figures 3.20(a)-(d) show the positions of the open curve at iterations 1, 8, 16 and 32 respectively.

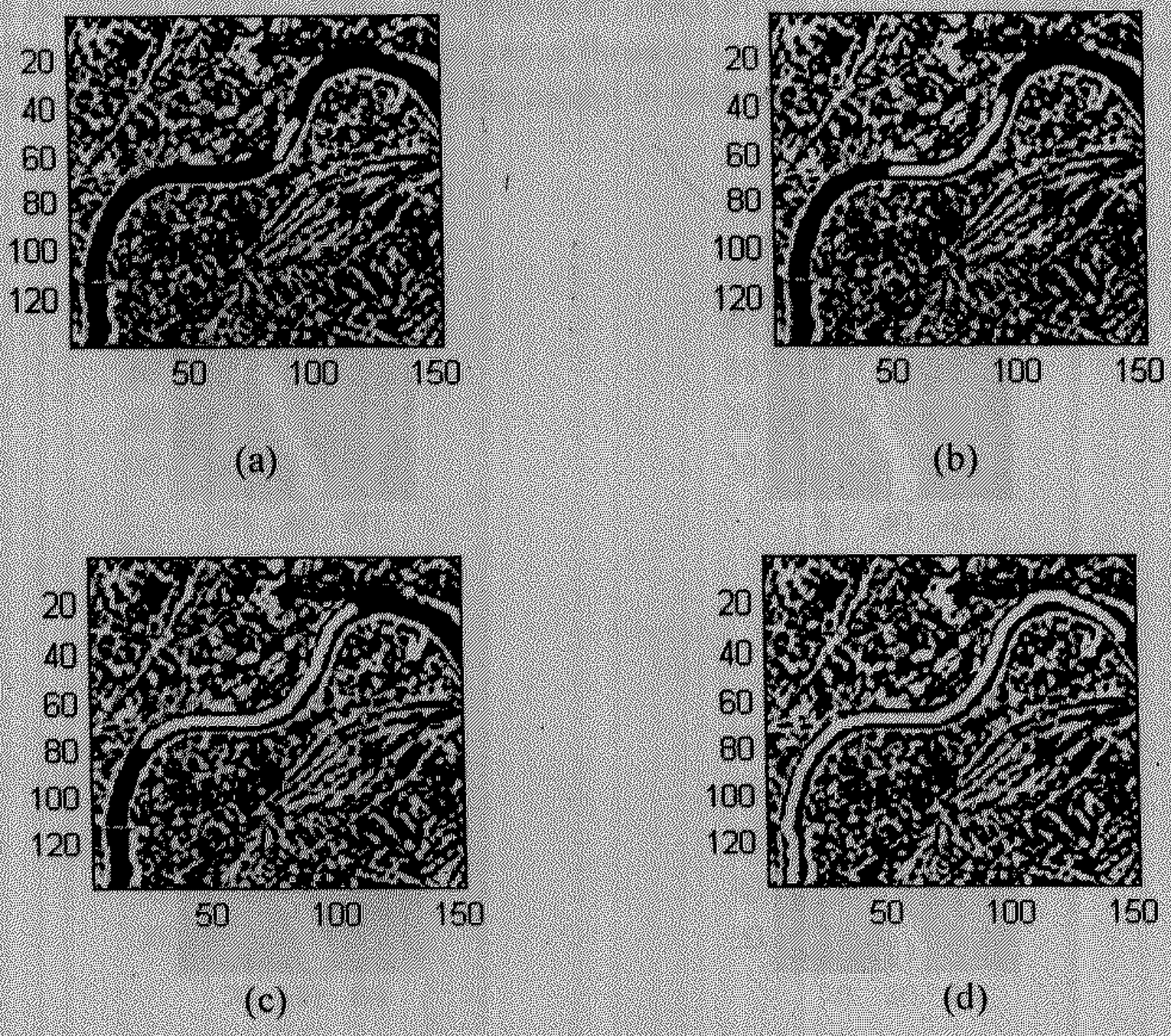

Figure 3.20: Result of applying equation (3.14) to a real 138×152 image of a satellite picture of a river. The river is identifiable as the thin black curve along the center. The yellow curve denotes the position of the open curve. (a) Iteration 1. (b) Iteration 8. (c) Iteration 16. (d) The curve has captured the shape of the river at iteration no 32.

4.8 DETECTING AN ARTERY FROM A REAL M.R.I IMAGE WITH THE MODEL IN SECTION 3.2

We have applied equation (3.14) in evolving a real 113×75 image of an MRI image of a brain artery. The artery is identifiable as the white filament along the center. Parameter values are same as in example 4.3. The open curve is initialized within the artery before start of calculations. Figures 3.21(a)-(d) show the position of the open curve in red at iterations 1, 6, 22 and 36 respectively.

It should be noted that the shape distortions or kinks in the image of the artery could not distract the growth of the open-ended curve through the entire process of evolution. This serves as a proof of the robustness of the model in section 3.2.

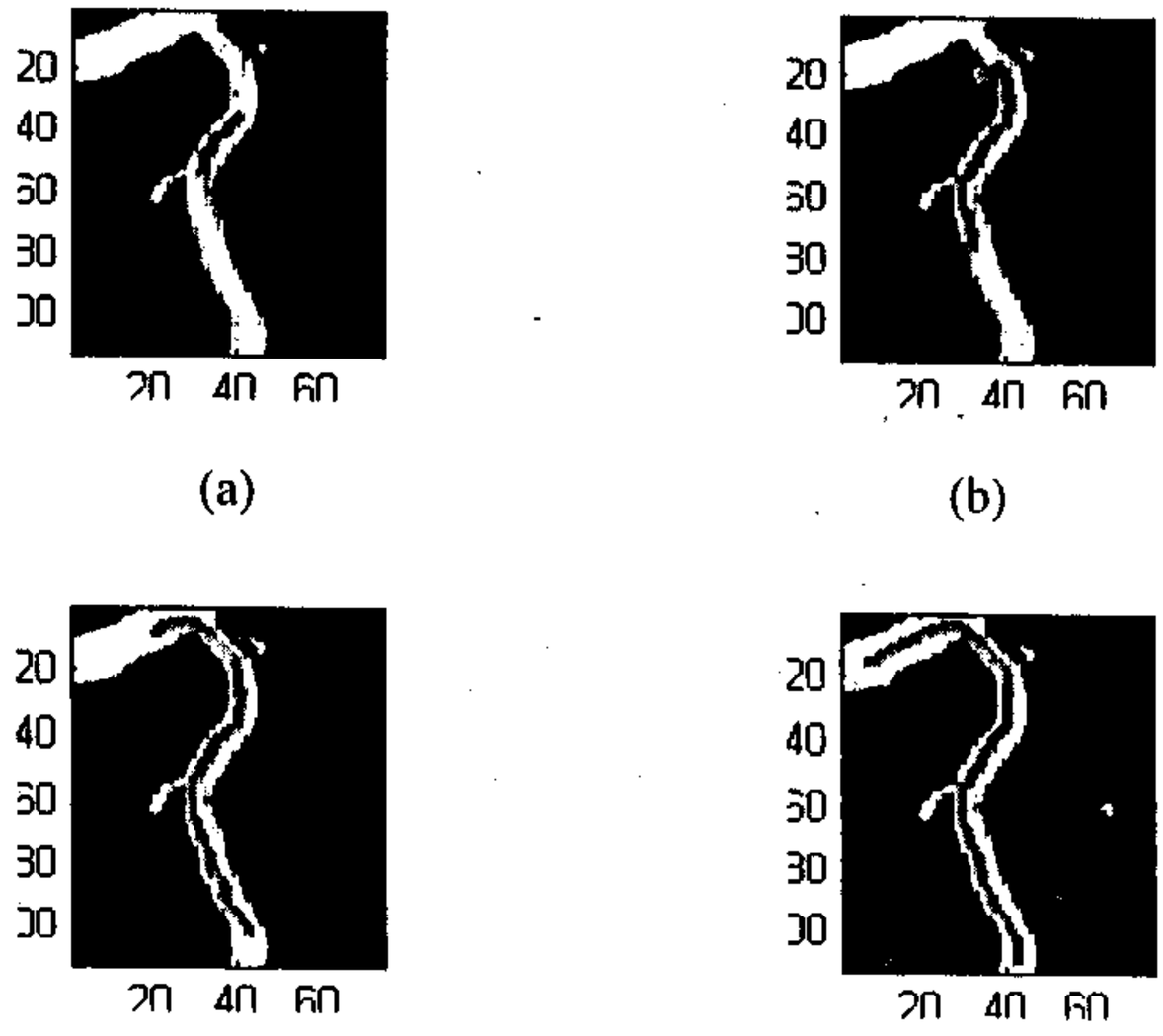

Figure 3.21: Result of applying equation (3.14) to a real 113×75 image of an MRI of a brain artery. The artery is identifiable as the white filament along the center. (a) The red curve denotes the position of the open curve at iteration 1. (b) Iteration 6. (c) Iteration 22. (d) The curve has tracked the artery at iteration 36.

4.9 IMPORTANT POINTS TO NOTE FROM EXAMPLES PRESENTED IN SECTION 4.1 TO SECTION 4.8.

It should be noted from the examples presented in sections 4.1-4.8 that the proposed curve evolution theory is efficient in segmenting one-dimensional shapes in synthetic as well as real images. It survives shape distortions or discontinuities of the filament edges and can grow undistracted (refer figures 3.21(a)-(d)). Even though an almost linear structure is used to initialize the open-ended curve, the curve can grow and follow the bending and twisting of the filaments that it attempts to segment (refer figures 3.16(a)-(d)). It can also adapt to local topologies, as in the case of dividing and following two different branches of the road in figures 3.17(a)-(d). It is also worthwhile to note the extent of elongation of the open curves and how smoothly it could adapt to image noise, shape distortions like bending, forking, etc and still retain its thin shape.

5. DIFFICULTY AND FUTURE WORK

The main problem in the new scheme introduced in section 3.2 is the choice of the time period of diffusion T in equation (3.10) or the width of the Gaussian kernel K in equations (3.11) and (3.14) (because they effectively reinitialize Γ before Γ starts to lose its elongated band-like structure and approach the shape of a circle). The critical threshold λ in equations (3.11) and (3.14) is also to be selected with great care as a very high λ may decrease the area of the reinitialized Γ (thus shortening the length of its medial axis), and a very low value of λ may cancel the effects of the anisotropic diffusion of Γ at the filament edges (thus creating isotropic diffusion of Γ across the filament edges). The proposed method also needs to be tested for robustness against noise in the image. A highly unsmooth forcing field $\vec{F}$ in equations (3.10) and (3.11) might break up the structure of the evolving Γ. This calls for critical choice of the weighing term η.

The next step includes the validation of the approach in section 3.2 with highly unsmooth forcing fields $\vec{F}$. Estimation and establishment of heuristics for the calculation of the parameters K in equations (3.11) and (3.14), T in equation (3.10), λ in equations (3.11) and (3.14) is a necessary requirement for the rigidity of this model. Establishing the mathematical characteristics of the type of motion induced by equations (3.11) and (3.14) is also a necessary step in the evolution of this theory as the motion characteristics will give us a better understanding of the internal mechanics of the whole process and hence a better control over the selection of the parameters. Application of this method to evolve open-ended curves in feature space to generate a non-linear boundary between different pattern classes may also be of interest.

6. CONCLUSION

We have introduced two new approaches to the problem of evolving an open-ended curve in a two-dimensional image plane. The first approach is an extension to the existing level set theory and is suitable for tracking the contours of objects in images with open curves that are possible with closed curves also. The second approach is a completely new visualization of the implicit representation of open curves in a 2D plane. This approach is particularly suitable for segmenting one-dimensional filament like structures in the 2D images. The second approach solves a segmentation problem (of 1D filaments) that was hitherto inefficiently catered to by the traditional level set method. Both the methods need to be tested for their mathematical characteristics and robustness to variations in input images. It is hoped that further research along the lines introduced in this thesis will achieve its goal of establishing a robust implicit mathematical theory for segmenting one-dimensional structures in 2D images with open-ended curves.

REFERENCES :

[1] L. Ambrosio, H. M. Soner, "Level Set Approach to Mean Curvature Flow in Arbitrary Codimension," J. Diff. Geometry, 43:693-737, 1996.

[2] P. Burchard, L. T. Cheng, B. Merriman, and S. Osher, "Motion of curves in three spatial dimensions using a level set approach," J. Comput. Phys., 170(2): 720-741, 2001.

[3] José Gomes, Implicit Representation of evolving manifolds in computer vision, Ph.D Thesis, submitted to the University of Nice – Sophia Antipolis, November 2001.

[4] L.M. Lorigo, O. Faugeras, W.E.L. Grimson, R. Keriven, R. Kikinis, A. Nabavi, and C.F. Westin, "Codimension-Two Geodesic Active Contours for the Segmentation of Tubular Structures," In *Proceedings of the International Conference on Computer Vision and Pattern Recognition*, Hilton Head Island, South Carolina, pages 444-451, June 2000.

[5] D.P. Mukherjee, N. Ray, and S.T. Acton, "Level set analysis for cell detection and tracking," IEEE Trans. Image Processing, 13(4): 562-572, April 2004.

[6] S. Ruuth, B. Merriman, J. Xin, and S. Osher, Diffusion generated motion by mean curvature for filaments, Technical Report 98-47, UCLA Computational and Applied Mathematics, Nov. 1998.

[7] S. Ruuth, B. T. R. Wetton, "A Simple Scheme for Volume Preserving Flow by Mean Curvature," Journal of Scientific Computing, Volume 19, Issue 1-3, December 2003.

[8] Guillermo Sapiro, Geometric Partial Differential Equation and Image Analysis, Cambridge University Press, Cambridge, UK, 2001.

[9] J.A. Sethian, Level set Methods and Fast Marching Methods, Cambridge University Press, Cambridge, UK, 1999.

[10] Chenyang Xu, Jerry L. Prince, "Snakes, Shapes, and Gradient Vector Flow," IEEE Trans. on Image Processing, Vol. 7, No. 3, March 1998.

[11] Hong-Kai Zhao, T. Chan, B. Merriman and S. Osher, "A Variational Level Set Approach to Multiphase Motion," J. Comput. Phys.,127, 179-195 (1996).